SAPIENZA UNIVERSITA' DI ROMA

Facoltà di Ingegneria
Corso di Laurea in Telecomunicazioni
Tesi di Laurea Specialistica

CIRCUS

Convergence of InfraRed Communications and Ultrawideband Systems

Relatore:
Prof. M. G. Di Benedetto
Correlatore:
Dr. L. De Nardis

Laureando:
Giorgio Corbellini
Matr. 795685

Anno Accademico 2006-2007

Summary

In recent years, wireless communications have gone through dramatic changes and evolved to decentralized systems that are not necessarily provided with infrastructure. In this scenario Ultrawideband (UWB) and Optical communications are two quite different transmission technologies that are used in different transmission contexts. Even though based on extremely different physical layers, UWB and optical signals share a fundamental feature i.e. the impulsive nature; in theory they may thus converge in a unique dual system giving rise to an extremely powerful wireless system able to work properly against interferers of different natures. This dual system would not need licenses to transmit thanks to the peculiarities of low power emissions typical of UWB technology and the use of optical signal that do not follow standard regulation rules since they do not interfere with electromagnetic waves.

Ultrawideband is a virtually carrier-less system which operate on a very large bandwidth. In recent years, it has received an increasing research interest and firsts UWB RF transmitters are available in USA, an example is the wireless USB Hub based on UWB technology released in 2006 by Belkin Corporation. Most of the research on UWB is related to RF UWB but UWB signals can, also be generated by emitting pulses very short in time. Theoretically if a dual physical layer system is present, if the impulsive UWB part of the system would perceive a too much high level of interference, switching to an optical physical layer could improve the

robustness of the entire system and would convoy an high degree of confidentiality provided that the optical radiation is essentially confined to the room where it is generated.

Within this framework network management and control protocols reflecting this paradigm are needed. The aim of this work is proposing a dual physical layer system and describing in a unified view both theoretical and basic research issues that integrate the potential of Ultrawideband and Optical Wireless Communications.

In Table 1 the principle peculiarities of a generic radio transmitter and an optical infrared system for indoor communications are reported and compared. As described in [1], radio and optical infrared are complementary transmission media, and the choice of the best medium is application dependent. Radio links are favoured in applications where user mobility must be maximized or transmission through walls or over long ranges is required, they are usually preferred when transmitter power consumption must be minimized. Infrared is favoured for short-range applications with a low degree of mobility, in which per-link bitrate and aggregate system capacity must be maximized or cost must be minimized. Signal confinement of optical transmissions naturally prevents from interference links operating in different rooms and secure against eavesdropping while in radio applications different techniques must be considered (such as channel coding) if a more secure system is wanted. Provided that both the technologies are pulse based, a suitable Medium Access Control (MAC) layer for the merging system should be specifically designed. In this work we chose to adopt the UWB^2[2] MAC protocol that is specifically designed for an impulsive UWB system but that can be theoretically exploited by a wireless optical system too.

Table 1. Comparison between radio and Intensity Modulation with Direct Detection (IM/DD) (optical) systems.

Property of Medium	Radio	IM/DD Infrared	Implication for IR
Bandwidth regulated?	Yes/ No(for UWB)	No	Approval not required. Worldwide compatibility.
Passes Through Walls?	Yes	No	Less coverage. More easily secured. Independent links in different rooms.
Multipath Fading?	Yes	No	Simple link design.
Multipath Distorsion?	Yes	Yes	
Path Loss	High	High	
Dominant Noise	Other Users	Background Light	Limited range.
Input $X(t)$ Represents	Amplitude	Power	Difficult to operate outdoors.
SNR Proportional to	$\int \lvert X(t)\rvert^2 dt$	$\int \lvert X(t)\rvert^2 dt$	High transmitted power requirement.
Average Power Proportional to	$\int \lvert X(t)\rvert^2 dt$	$\int \lvert X(t)\rvert dt$	Choose waveform $X(t)$ with high peak-to-average ratio.

Both optical infrared and UWB techniques will be separately analyzed, key aspects of the different technologies will be remarked and all the analogies will be exploited for the definition of the converging system. Chapter 1 is dedicated to the description of optical systems, in particular principal elements of an optical wireless communications system are underlined. In chapter 2 we introduce the UWB technology and we focus our attention on the TH-PPM UWB system describing the transmitted signal, its spectrum and the power constraints it is subject to. Chapter 3 contains the description of the converging system, physical layer analogies are analyzed and different switching strategies are proposed. Simulation results and

conclusions represent the content of chapter 4.

Acknowledgements

Desidero ringraziare i miei genitori Luciano e Valeria e dedicare a loro questo mio lavoro. Con il loro costante aiuto, fatto di telefonate comprensive e di qualche visita fugace hanno saputo rendere decisamente meno duro questo mio percorso caratterizzato, come mia abitudine, dal voler fare contemporaneamente molte più cose di quelle che dovrei complicandomi non poco la vita. Un ringraziamento speciale va a Sabina, una splendida realtà, che mi ha supportato nei momenti difficili sapendomi dare la sicurezza necessaria per poter continuare al meglio, che oramai dopo tanti anni sa esattamente cosa dirimi al momento giusto e con la quale ho condiviso dei momenti indimenticabili. Grazie. Non posso di certo non ringraziare i miei fratelli, Alberto, Viola e Filippo che non sono mai mancati quando avevo un problema e che mi hanno sempre incoraggiato. Ringrazio i miei amici, Paolo, Paola, Federica e tutti gli altri con i quali ho condiviso questi bellissimi anni di università fatti di bei momenti di divertimento ma anche di tremende nottate passate a studiare insieme a casa di qualcuno di noi. Grazie al mio Relatore, la Prof. Di Benedetto che ha creduto in me e che mi ha dato la possibilità di realizzare questo lavoro. Grazie anche al mio Correlatore, il Dr. De Nardis che nonostante la mia invadente ed insistente richiesta di spiegazioni mi ha sempre puntualmente risposto.

Contents

List of Tables

List of Figures

Chapter 1

Optical Communications

1.1 Historical Overview & State of the Art

Since ancient times light has been used to convey information from source to destination. Fires, torches, and the reflection of sunlight over a mirror, have been used, for example, to transmit alerts of approaching dangers such as enemy armies. A human observer acted as the receiver by visually perceiving optical signals. In more complex systems, the transmission process included information coding, as in navy flags for example, where a person waves arms or flags in different patterns to represent letters and numbers. The introduction of mechanical tools allowed shapes and patterns to grow larger and, therefore, be identified by an observer at larger distances than with human transmitters. The first significant example adopting this strategy was invented in the 1790's by French engineer C. Chappe and was named optical telegraph (see Figure 1.1). The system, consisting in a series of semaphores mounted on towers where human operators relayed messages from one tower to the next, was much faster than hand-carried messages, but was replaced by mid-19th century by the electric telegraph, leaving a scattering of "Telegraph Hills" as its most visible legacy.

After the electrical telegraph was established, J. Leseurre introduced in 1855 the

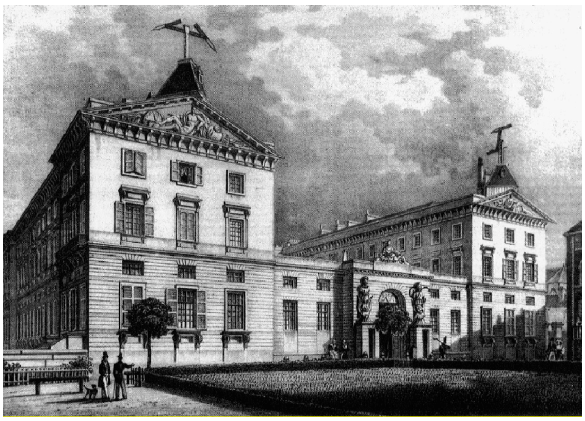

Figure 1.1. Optical telegraph station at Metz, France (about 1830).

mirror heliograph that is a system capable of transmitting light beams after multiple reflections of sunlight over a set of mirrors in the direction of an intended recipient. The beam was keyed "on" and "off" by means of a shutter or tilting mirror, and allowed thus the transmission of Morse coded messages. The system was operated at a speed of 5 to 12 words per minute, depending on Morse skills of the operator. During late 1800's, heliographs were used in several countries, typically for military applications.

Another breakpoint in the history of optical communications was the discovery of the phenomenon known as total internal reflection that is the confinement of light in a material surrounded by a medium with lower refractive index, such as glass in air. In the 1840's, D. Colladon and J. Babinet showed that light could be guided along jets of water for fountain displays. J. Tyndall popularized light guiding in an experiment that he first demonstrated in 1854, in which light was guided in a jet of water flowing from a tank (see Figure 1.2).

As regards the use of light for data transmission, it is as back as in 1880 that

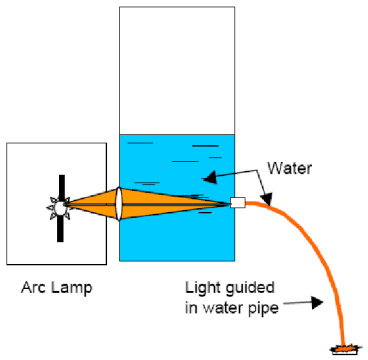

Figure 1.2. The Tyndall experiment.

A. G. Bell patented an optical wireless telephone system called the Photophone. Bell dreamed of sending signals through the air, but experienced that the atmosphere did not transmit light as reliably as wires carried electricity. In the following decades, light was used for very limited and specific applications, as for example signalling between ships, and optical communication systems, such as the experimental Photophone donated by Bell to the Smithsonian Institution, languished on the shelf.

The next important milestone was reached in 1958, about 80 years after the Photophone, when L. Schawlow and C. H. Townes published their theoretical results on the possibility of amplifying light by stimulated emission of radiation. In their study, Schawlow and Townes were actually considering microwave frequencies, but their results opened the way to investigations in the infrared and visible spectrum. This concept later formed the basis for the development of laser devices. As a natural consequence, research and development intensified for creating practical devices, and it was in 1960 that T. Maiman invented the first ruby-based practical laser (see Figure 1.3). The device was identified as a possible emitter in wireless optical communication systems, since air is far more transparent at optical than

at millimeter wavelengths. It was, however, soon realized that rain, haze, clouds, and atmospheric turbulence limited the reliability of long-distance atmospheric laser links. By 1965, it was clear that major technical barriers remained for both millimeter wave and optical wireless communications. In the meanwhile, optical fibers had attracted attention given their analogy, in theory, to plastic dielectric waveguides used for microwave applications. At this time, the scientific community considered, however, fibers to be too lossy for communication purposes, due to the large attenuation values experienced by propagating waves, and fibers were confined to applications that required coverage of short distances such as in medical applications for exploring the human body.

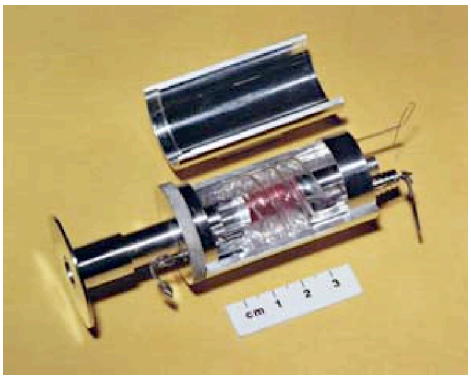

Figure 1.3. The Maiman Laser.

Nevertheless, a few researchers still believed in the fiber as a possible transmission medium for long-range communications. Among them was a team at Standard Telecommunications Laboratories, initially headed by A. E. Karbowiak, and then by C. K. Kao. This group focused on reducing fiber attenuation by carefully investigating the properties of glass. Results of this investigation showed that the high losses characterizing fibers were mainly due to the presence of impurities and not to silica glass itself. Kao defended his PhD thesis in 1966 and discussed the hypothesis of

using, in theory, single-mode fibers with attenuation below 20 dB/km for long-range communications. The first usable optical fiber was invented in 1970 by researchers R. D. Maurer, D. B. Keck, P. Schultz, and F. Zimar working for American glass maker Corning Glass Works (see Figure 1.4). They manufactured a fiber with an attenuation of 17 dB/km, by doping silica glass with titanium. Based on this discovery, the first experimental fiber optic communication system was installed in 1976. Using a gallium-arsenide semiconductor laser, the AT&T US company installed an experimental 2000-meter-long (1.25 miles) fiber optic cable under the streets of Atlanta, Georgia. The technology evolved so fast that in 1980 with similar emitters the degree of purity of the fiber allowed a 240 km coverage; if the sea was as transparent as such a fiber, one would see the bottom of the Pacific ocean as clearly as in a pool, even in the deepest abyssal zones. By mid-80's, the fiber replaced wired-copper, microwave and satellite links. The first transatlantic telephone cable using optical fibers named TAT-8 was put in operation in 1988 by AT&T. It initially carried 40,000 telephone circuits (simultaneous calls) between the US and France, offering a capacity of (2+1)x280 Mb/s, indicating that two fibre pairs with a capacity of 280 Mb/s each were available to provide normal service, while another fibre pair with similar capacity was available for back-up purposes .

At this stage, amplification was electrical. Performance i.e. signal-to-noise, was mainly limited by amplifiers rather than by lasers and fibers. The evolution towards systems covering larger distances at higher transmission rates could be made possible by reaching pure optical amplification. In 1985, S. B. Poole, from Southampton University, UK, discovered that it was possible to create a full-optical amplifier by doping glass fibers with Erbium. Using this approach, D. Payne and P.J. Mears, also from Southampton University, and E. Desurvire from the Bell Laboratories, developed a full-optical fiber link.

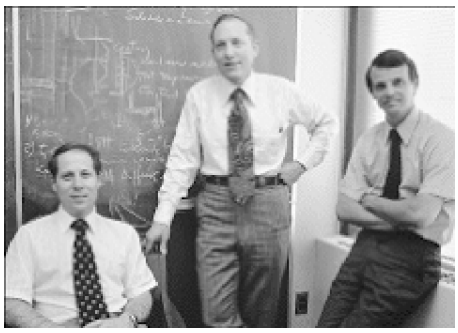

Figure 1.4. Donald Keck, Robert Maurer, and Peter Schultz from Corning Glass Works, creators of the first practical optical fiber. (Photo from Corning Glass Inc.)

In the 90's, cable television adopted fiber optics to enhance network reliability. Computers and Local Area Networks (LANs) started using fiber at about the same period of time. Industrial links were among the first to be set, since features such as noise immunity and low attenuation made it ideal for factories and storage networks. Several other applications developed fast: on-board aircraft and satellites copper cable replacement thanks to the reduced weight, ships and automobile data buses, surveillance systems for security, links for consumer digital stereo, etc.

Today's fiber transmission standard rates could be reached thanks to the introduction of multiplexing, and in particular Wavelength Division Multiplexing (WDM) techniques. In a similar way of Frequency Division Multiplexing (FDM) for Radio Frequencies (RF) channels, WDM allowed for the transmission of different wavelengths of light simultaneously over a single fiber, maximizing thus the total bandwidth per fiber. Systems such as TAT-14 entered the service by the end of 2000, offering a capacity of (4+4)x160 Gb/s (over 1500 times more capacity than 12 years earlier with TAT-8).

In the recent past, the possibility of using wireless optical transmissions, also referred to as free-space optical communications (FSO), as an alternative (or a supplement) to fiber optics connections came back to surface. The main reason for this interest is the possibility to have a license-free high-speed link where cable transmissions will be logistics difficulties for deploying the fiber. FSO and fiber transmissions use similar light wavelengths, reach similar transmission bandwidths, and adopt similar modulation techniques. Point-to-point broadband wireless optical connections with transmission rates up to 1 Gb/s are nowadays practicable. A common scenario of application for FSO consists in wideband connections between two points, for example two buildings, where the installation of a wired connection would either be impossible or too expensive, and where a microwave radio based system would not offer the necessary bandwidth (see Figure 1.5). Well-designed FSO systems are typically characterized by outage probability of 10^{-3} at 500-2000 m ranges, and have been installed in several cities all around the world for example in the surrounding area of Milan, in Italy [3] . A feasible use of an FSO system is the installation of the "last mile" link from the fiber backbone directly to the client or between different buildings [4]. FSO system performance is primarily dependent upon the climatology and physical characteristics of the installation location. Even if modern systems can work with every kind of climate [5], atmospheric attenuation typically dominated by fog, low clouds, rain, snow and dust is the major weakness of this systems. Turbulences can also cause atmospheric scintillation, which introduces fluctuations in the received light intensity. Alignment between transmitter and receiver is another key factor; FSO emitters transmit in fact highly directional and narrow light beams that must impinge upon the aperture of the receiver. A typical FSO emitter transmits one or more light beams; each of these is about 5-8 cm in diameter at the transmitter and typically spreads to roughly 1-5 m in diameter at a range of 1 km. This effect might prove to be disastrous when, for instance, either the transmitter or the

receiver moves unexpectedly, even by a slight amount. Buildings, for example, are constantly in motion due to a variety of factors, including thermal expansion, wind sway, and vibration. Because of the narrowness of the transmitted beam and the restricted receiver Field Of View (FOV), building sway can affect link alignment and interrupt communication. Since FSO systems can be easy installed they can be used in mobile/nomadic situations (e.g seminars, meetings or events) but also the creation optical bridges between different locations for disaster management is a possibility.

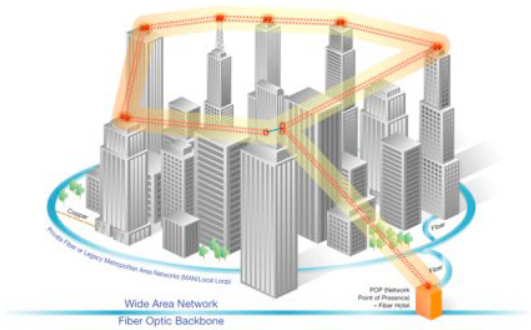

Figure 1.5. Example of a FSO system interconnecting different buildings to the fiber backbone.

A different scenario of application for wireless optical transmissions consists in communications based on light diffusion. These systems are suitable for low/medium baud-rates links for cable replacement, with a small degree of mobility. Optical wireless links between portable devices, as well as for in-house applications, have been a hot research topic [6],[7],[1],[8],[9],[10], in parallel with the development of RF solutions in the same framework. In diffuse systems, the link is always maintained between any transmitter and any receiver in the same vicinity by reflecting the transmitted information-bearing light off reflecting surfaces such as ceilings, walls and furniture. The transmitter and the receiver are not necessarily in visibility, thus

Non Line-of-Sight (NLOS) links are fully exploited. Table 1.1 summarizes the main properties of directed and diffuse links.

Table 1.1. Main Properties of the basic optical wireless links.

Type of link	Tx FOV	Rx FOV	Connection	Advantage	Disadvantage	Implementation
Directed	Narrow	Narrow	LOS	High speed	Shadowing	Complex
Diffuse	Wide	Wide	Reflections	High Coverage	Low speed	Simple

Diffuse systems are mainly used for indoor transmissions and the diffuse optical channel is exposed to ambient light sources like daylight, tungsten light and fluorescent lamps. In general, there is an high level of stationary or slowly fluctuating ambient light generating shot noise in the receiving photodiode. In addition, artificial-light sources also emit rapid fluctuating components associated with higher harmonics of the mains frequency; this have to be eliminated by electrical filtering. Part of the incidental ambient light can be mitigated by optical filtering.

Nowadays, there is no real competition between wireless RF and wireless optical systems. RF systems are well established, cheap and robust, but there are some specific scenarios in which wireless optical systems may be competitive. F.R. Gfeller [6] proposed for example using infrared systems as an alternative to RF for portable terminals in indoor applications. An interesting use of optical diffuse systems that is becoming popular is Visible Light Communication (VLC) that is communicating via 380-700 nm LEDs, due to the inherently diffuse optical source, the safety issue is minimized. Furthermore provided that the emitted light is visible those systems could be used simultaneously lighting and communication. The idea of bringing these two worlds together was recently re-invigorated through the emergence of white-light LEDs, which offer a considerable modulation bandwidth of about 20

MHz [8] and are low cost elements [11]. As a matter of fact, several manufacturers and research groups produce nowadays wireless optical products for a wide range of applications. Nowadays optical communications are integrated into the communication world thanks to the definition of standards classified in correspondence to channel types that is fiber, FSO, and diffuse optical wireless.

Communication networks that use the fiber as the transmission medium. There are several standards developed by international organizations for different application scenarios. The North American Telecommunications Industry Association (TIA) has promoted the FO-4 Engineering Committee on Fiber Optics as a responsible for the development and maintenance of fiber optic components, subsystems, systems, and network technology standards. For example a sub-committee of FO-4 established that the recent TAT-14 submarine transatlantic cable system should use WDM with 16 wavelengths per fiber pair, giving an aggregate capacity of about 9,700,000 circuits per fiber. Other standards are promoted by the IEEE and OSA (Optical Society of America): these were adopted for several applications such as cable TV and hybrid networks, LAN, Metropolitan Area Network (MAN), and Wide Area Network (WAN), Synchronous Digital Hierarchy (SDH) networks, submarine links.

FSO Free space optical systems are not intended to be standardized.

Diffuse Wireless Optical (DWO) For Diffuse Wireless optical systems two main commercial standards are available: the IrDA standard for computer and peripherals interconnection (also used for connections between cellular phones or palm computers) and the IEEE 1073 standard for medical instrumentation interconnection.

1.1.1 Basic Concepts in Optics

Light is an electromagnetic radiation characterized by periodically varying electric and magnetic fields that are mutually orthogonal and move at the speed of light. When travelling through space or being reflected, light behaves like a wave. When emitted from, or absorbed by, materials, it behaves like a particle. As a general concept, an electromagnetic radiation is characterized by three parameters (amplitude, wavelength or frequency, and phase). Wavelength is defined as "the distance over which the wave repeats itself" and is represented by λ. The time required to complete one cycle of the wave, is called period of the wave. The frequency of the wave is the number of cycles of the wave contained in one second and is represented by ν. Electromagnetic radiations are classified as a function of their wavelength; the infinite possible values of wavelengths, and corresponding radiations, are commonly referred to as the electromagnetic spectrum (see Figure 1.6) .

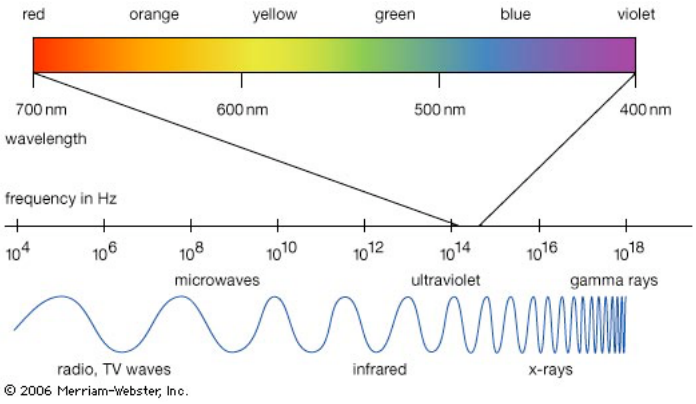

Figure 1.6. The electromagnetic spectrum.

As it is shown in the Figure we can classify radiations with respect to the increasing frequencies (reducing wavelengths):

- radio waves in the region of wavelengths between 300'000 and 0.3 meters, corresponding to frequencies between 1 kHz and 1 GHz)
- microwaves, wavelengths from about 0.3 meters to about 0.0003 meters
- infrared from about 300 to 0.7 μm
- visible light, from 0.4 to 0.7 μm
- ultraviolet from about 0.4 to 0.01μm
- x-rays from about 0.01μm to about 10E-4μm
- gamma rays, wavelengths shorter than about 10E-4μm

These last very short-wavelength, high-energy radiations show interactions with the matter that are more particle-like than wave-like. Indeed, gamma rays are usually characterized in terms of their photon energy, above 10^3 keV (Gamma rays are the most energetic form of electromagnetic radiation). In the following, we will focus on the so-called optical spectrum including infrared, visible and ultraviolet:

- Infrared (IR) is the portion of the electromagnetic spectrum with wavelengths from about 300 to 0.7 μm (over the red part of the visible light). It can be further subdivided into far, intermediate and near infrared. Far and intermediate infrared, corresponding to the longer wavelengths, are used for thermal imaging, while the near infrared region is useful not only for optical communications but for detection and identification of superficial materials.
- Visible light (VIS) is the rather narrow but important region of the electromagnetic spectrum to which the typical human eye is sensitive. It goes from the red (near to infrared) to the blue (near to ultraviolet).

- Ultraviolet (UV) is a more energetic electromagnetic radiation that covers the region from about 0.4 to 0.01 micrometers. It is capable of inducing photochemical reactions and is generally detrimental to organic materials. Far UV is strongly absorbed by ozone, (also by oxygen) and is also strongly attenuated by normal glass lenses.

The transmission characteristics of several materials as well as the absorption for different atmospherical components in the near infrared region have been extensively analyzed. As a result of this analysis, three wavelength regions have been identified, that are characterized by a low attenuation. These regions are called transmission windows. The first window has wavelengths between 700 and 900 nm; the second includes wavelengths from 1200 to 1300 nm, while the third one is centered around 1550 nm. The existence of such transmission windows has driven the design of emitters and receivers, that typically operate in one of the windows.

1.1.2 Properties of the Light

Polarization As mentioned above, light consists in wave variations of mutually orthogonal electric and magnetic fields. As a consequence, if the direction of one of these fields is known, the direction of the other is also known. The polarization of light defines the orientation of the electric field in space. The following terms are commonly employed in the description of polarized light:

- Unpolarized light has no specific orientation of electric field. The direction of the electric field varies randomly at approximately the frequency of light.

- Plane-polarized light is characterized by an electric field that oscillates in one plane only.

- In vertically-polarized light the plane of the electric field is vertical and moves

up and down in the plane. In horizontally-polarized light the plane that contains the electric field is horizontal.

- In circularly-polarized light, the direction of the electric field is neither random nor confined to a single plane. The direction of the electric field of circularly-polarized light sweeps out a circle during each period of the wave.

Coherence Can be defined for light waves as the condition that exists when all the light waves are in phase. The coherence can be defined as follows: if we consider a set of light waves emitted at the same instant in the same point in space, these light waves are temporally coherent if, given an observation point in space and an observation instant in time, all the light waves show the same value of the electrical field. In the case of a light source, there are two main causes of lack of coherence:

- **Temporal** The variation of the electrical field in a light wave depends on the frequency (or, equivalently, wavelength) of the light wave. Since an optical source emits several light waves at the same time, the more nearly the output of the source approximates a single frequency (monochromaticity), the more temporally coherent is the emitted light.

- **Spatial** A light source emits arrays of photons (each of them corresponding to a light wave), that are supposed to depart at the same time by the entire area of emission. In a light source characterized by a large active area of emission, however, different sections of the area of emission will emit photons belonging to the same array in different times, causing a lack of coherence. As a consequence, the smaller is the extent of a light source, that is the more it resembles a *point source*, the greater the coherence of the emitted light.

Interference It occurs when a coherent light beam is divided into two parts and later recombined. If the two waves are combined at a point at which they are 180°

out of phase, the two electric fields cancel through a process called destructive interference producing a dark area. If both waves arrive in phase we have a constructive interference, and their electric fields add to produce an area that has an increased irradiance. If the two waves are of equal amplitude, the irradiance at this point is four times that produced by either of the beams alone.

1.1.3 Magnitudes and Units

In this section we shall briefly describe the units and magnitudes that are commonly used in optical communications. We will focus on the international system of units (usually called the SI, using the first two initials of its French name Système International d'Unités) The SI is maintained by a small agency in Paris, the International Bureau of Weights and Measures (BIPM, for Bureau International des Poids et Mesures).

Luminous intensity Also known as candlepower is the light density emitted within a very small solid angle, in a specified direction. The unit of measure is candela (cd). In modern standards, the candela is the basic of all measurements of light and all other units are derived from it.

Formally the *Candela* is defined to be the *luminous intensity of a light source producing single-frequency light at a frequency of 540 THz with a power of* $(\frac{1}{683 \cdot W/steradian})$*, or 18.3988mW over a complete sphere centered at the light source* (a steradian is defined as the solid angle that, given a sphere of radium R, determines on the surface of the sphere a circle of area R^2). The frequency of 540 THz corresponds to a wave length of approximately $555.17nm$. In order to produce 1 candela of single-frequency light of wavelength λ, a lamp would have to radiate $(\frac{1}{683 \cdot V(\lambda) \cdot W/steradian})$, where $V(\lambda)$ is the relative sensitivity of the eye at wavelength λ. These values are defined by the International Commission on Illumination (CIE).

Luminous flux It corresponds to the time rate of flow of light. The unit of measure is the lumen (lm). One lumen may be defined as the light flux emitted in one unit solid angle by a one-candela uniform-point source. The lumen differs from the candela in that it is a measure of light flux irrespective of direction. In fact, one lumen equals to the intensity in candelas multiplied by the solid angle in steradians into which the light is emitted. Thus the total flux of a one-candela light, if the light is emitted uniformly in all directions, is 4π lumens. Note that a lumen is a measure of optical power, as Watt is. The difference between lumen and watts relies in the fact that lumen definition takes into account the human eye sensitivity. Therefore, lights with the same power in watts, but different colours have different luminous fluxes, because the human eye has different sensitivity at different wavelengths. At a wavelength of 555 nm (maximum eye sensitivity) 1 Watt equals 683 Lm.

Very powerful sources of infrared radiation produce no lumen output, because the human eye can not see it. However, if you need to calculate total power absorbed by a surface (to estimate temperature increase, for example), you have to transfer lumen flux to watt. This can be done by using a spectral luminous efficiency curve ($\mathrm{V}(\lambda)$).

Illumination Illumination is defined as the density of luminous flux on a surface. This parameter shows how "bright" the surface point appears to the human eye. The SI unit to measure illumination is lux (lx) and is defined as an illumination of 1 lm/m^2.

Luminance or Brightness It is defined as the luminous intensity on a surface in a given direction per unit of projected area of the surface. Luminance is especially important because our eye only sees brightness, not illumination. It is proportional to the object's illumination, so a well illuminated object seems brighter. Luminance can be expressed in many ways: using SI units we can express it in candelas per

unit of area or in lumens per unit of solid angle per unit of area. In the CGS system we find the lambert (La) that is defined as the luminance of a surface that emits or reflects one $lumen/cm^2$. As it is a large unit, practical measurements tend to be in millilamberts (mLa). A surface area having an intensity of 1 cd/m^2 emits a total light flux of ($\pi \cdot \frac{lm}{sr/m^2}$); as a result: 1 La=3183.099 cd/m^2.

Lambertian Surfaces It is a diffuse reflector ideal. It is a surface that adheres to *Lambert cosine law*, that states that the reflected or transmitted *luminous intensity* in any direction from an element of a perfectly diffusing surface varies as the cosine of the angle between that direction and the normal vector of the surface. As a consequence, the *luminance* of that surface is the same regardless of the viewing angle. A good example is a surface painted with a good "matte" or "flat" white paint. If a Lambertian surface is uniformly illuminated, like from the sun, it appears equally bright form whatever direction you view it.

Lenses and Collimators Lenses are used in optical communications to change the direction of rays of light (see Figure 1.7). Lenses are used for example for separating different spots of light in order to avoid interferences, or for concentrating light on a point in order to increase the active area at the receiver without increasing other related parameters (as the spurious capacitance that severely limits the bandwidth at the receiver). They can be used also as filters for avoiding the incidence of signals out of the desired scope of wavelength. The effect of a lens on light is embodied in Snell's law of refraction. This law states that, in passing from a rarer medium into a denser one, light is refracted toward the normal. In passing from a denser to a rarer medium, light is refracted away from the normal. The degree of bending or refracting is in accordance with the following equation:

$$n_1 \cdot sin\theta_1 = n_2 \cdot sin\theta_2 \tag{1.1}$$

Where n_1 and n_2 are the indices of the two media, and θ_1 and θ_2 are the angles of incidence and refraction, respectively.

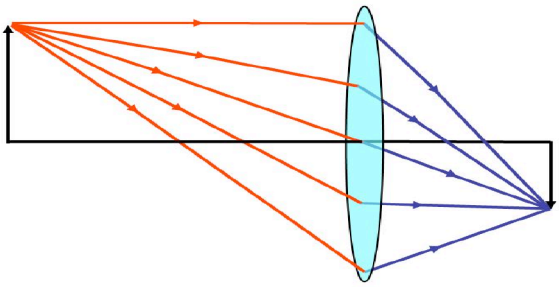

Figure 1.7. Image formation by simple lens.

Lenses can be classified into two general types according to the effect they have on a parallel beam of light. The two types are converging and diverging lenses.

Converging lenses Also are called "positive", "plus", or "convex" lenses. They are thicker in the middle than at the edges. They cause both parallel rays of light and diverging rays of light arriving at one side of the lens to converge on the opposite side.

Diverging lenses Also known as "negative", "minus", or "concave" lenses and are thinner in the middle than at the edges.

Diverging lens causes parallel rays of light to diverge or spread in opposite directions on the other side of the lens. If rays initially are diverging toward such a lens, they will be made to diverge even more strongly after they pass through the lens. Further subdivisions of these two basic types can be made according to the curvature of the lens surfaces. Spherical lenses are lenses whose surfaces are spherical in shape. They can be classified into the six sub-types shown in Figure 1.8. The

biconvex lens is the most used.

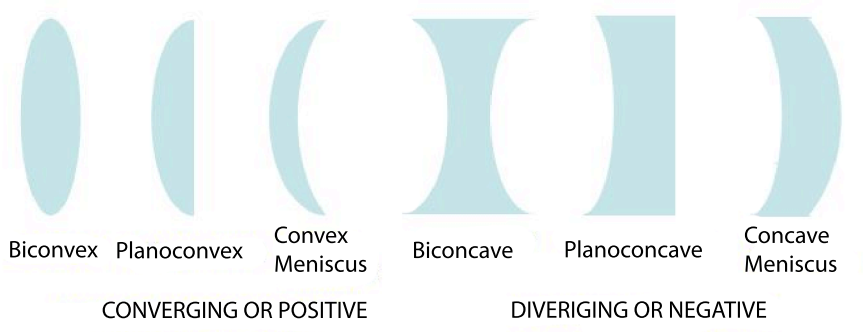

Figure 1.8. Types of simple spherical lenses.

A lens is characterized by the position of its focal point. The focal point F' (Figure 1.9) of a positive lens is that point where parallel rays of light from the left are brought together. The focal point F on the left side of the positive lens is that point to which parallel rays, incident on the lens from right-to-left, would converge. The focal point F (Figure 1.10) of a negative lens is the point where diverging rays of light generated from parallel incident rays seem to originate. The focal point F' on the right side of the lens is the point from which rays of light would seem to diverge, after passing through the lens, if they were incident on the lens from right-to-left.

The focal length of a lens is then defined as the distance between the focal point and the vertical centerline of the lens. Focal lengths are shown as f' and f in Figures 1.9 and 1.10 for a thin lens, f and f' are equal. The power of a lens is the reciprocal of its focal length in meters. The power of a lens is a measure of its ability to converge or diverge light rays: the higher the positive power, the more converging the lens. The unit of power is the diopter that is usually designated as D. *One diopter is the power of a lens with a focal length of one meter.* Note that a lens that causes light to converge has a positive power, and a lens that causes light to diverge has

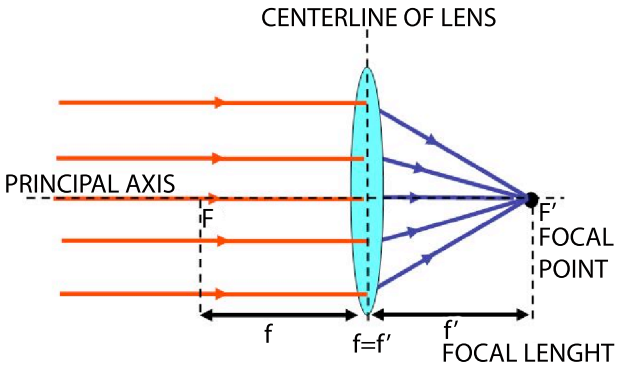

Figure 1.9. Parallel rays of light brought to a focus by a positive thin lens.

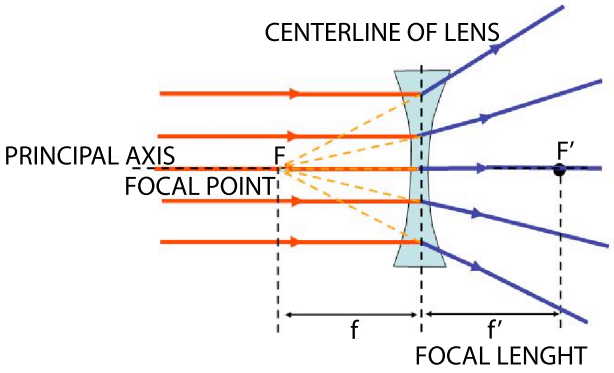

Figure 1.10. Incident rays on a negative thin lens (diverge as if coming from a point F on the left).

a negative power. The above definitions are valid for lenses where the thickness of the lens is negligible if compared with the focal length ("thin lens"). This condition is usually met by the lenses used in optical communications.

1.2 Concepts of optical communications

The general scheme of an optical communication system can be depicted as in Figure 1.11. The input to the system is a digital, base-band data signal. The data input is first processed in an electrical form at the transmitter by the transmitter electrical processor, secondly transduced into an optical signal by the optical emitter, and finally filtered and amplified by optical lenses. The output of the transmitter forms the input to the optical channel. At the output of the channel the optical signal that enters the receiver is corrupted by noise and interference. The receiver is formed by a front-end optical filter and amplifier, followed by a receiver transducer (the photodiode) that produces an electrical current that is processed by the final-stage amplifier and treated as any electrical signal would be. In this section we briefly analyze basic concepts related to the main blocks of Figure 1.11 and in particular: modulation and coding carried out by the transmitter electrical processor (section 1.2), transduction by the optical emitter (section 1.2.1), transmission over a real optical channel affected by noise and interference (section 1.2.2), transduction by the optical receiver (section 1.2.3), and amplification in the receiver electrical processor (section 1.2.3). Optical filtering and amplification by lenses have already been analyzed in the previous section.

Modulation and Coding

Modulation and coding schemes best suited for optical transmissions are commonly based on intensity modulation/direct detection (IM/DD) schemes operating either in the baseband or in shifted bands using electrical subcarriers. The information is then conveyed by the instantaneous optical power at the output of the optical emitter. At the receiver, a photodetector produces a current proportional to the received instantaneous optical power. This optical power is proportional to the square of the received electric field and is the integral over the photodetector surface of the

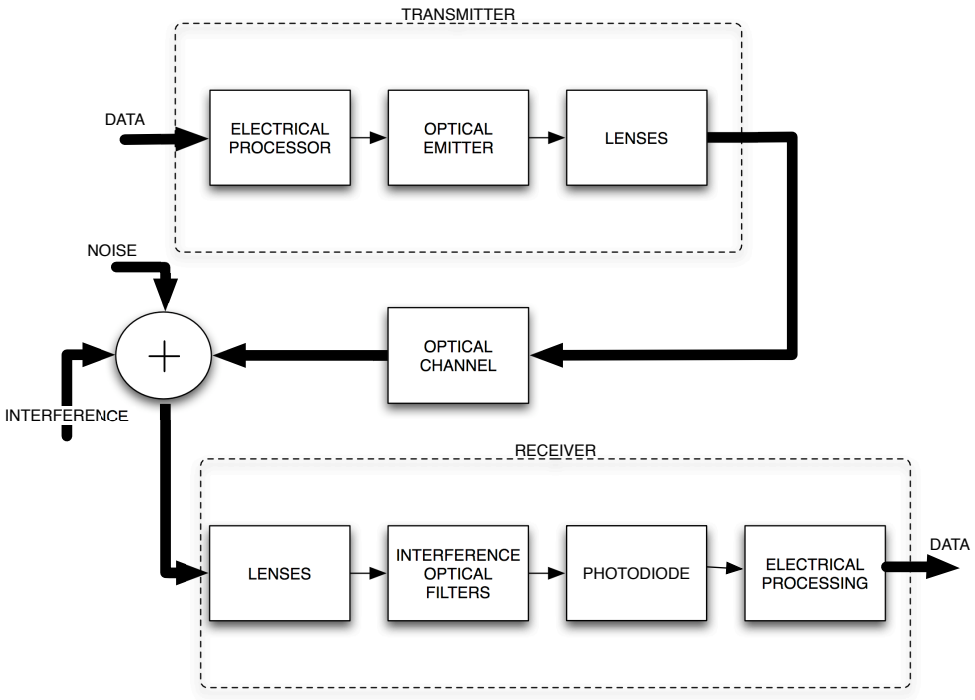

Figure 1.11. General scheme of an optical communication system.

received scattered optical power, similarly to what happens in a receiving antenna. Popular baseband modulation schemes are On-Off Keying (OOK) with Non Return to Zero (NRZ) and Return to Zero (RZ), Pulse Position Modulation (PPM). In Figure 1.12 these different binary modulation schemes are depicted: (a) in OOK with NRZ, (b) OOK with RZ with a duty cycle of γ=0.5, (c) 2-PPM, and (d) BPSK subcarrier at a frequency equal to the reciprocal of the symbol duration.

For all baseband and single-carrier modulation schemes, we define B the first null bandwidth of the Power Spectral Density (PSD) of the transmitted waveform $X(t)$. For multiple-subcarrier schemes, the bandwidth requirement B is the span from dc to the first null in the highest-frequency subcarrier. We will present bandwidth requirements B/R_b, i.e., normalized to the bit rate R_b. In Figure 1.13 the normalized spectrum of the four different binary schemes is provided. The power P_t is the

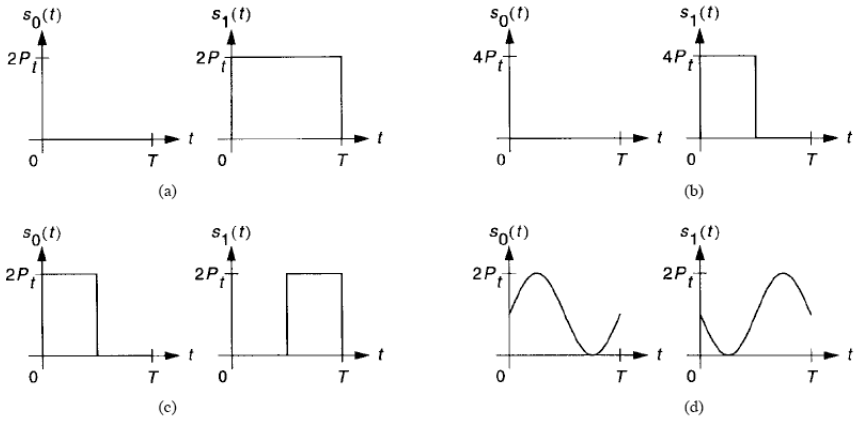

Figure 1.12. Common binary modulation schemes.

average transmitted optical Power, and T is the symbol interval (equal to the bit interval). The shown spectrum is referred to a transmitted signal of the form:

$$X(t) = \sum_{n=-\infty}^{\infty} s_{k_n}(t - nT) \tag{1.2}$$

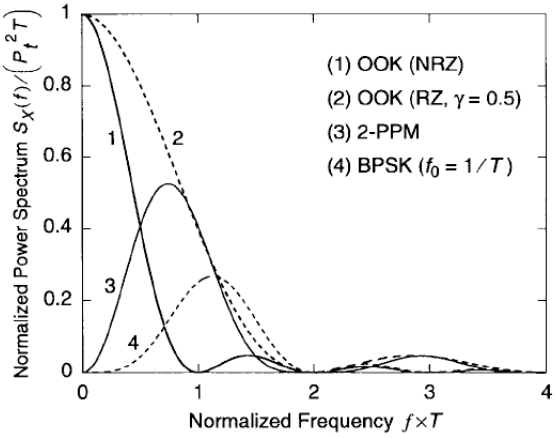

Figure 1.13. PSD of common binary modulation schemes.

OOK Is the simplest modulation scheme to implement [12] for optical communications, since, when noise is AWGN (and there is no multipath distortions), it

only requires an ideal maximum-likelihood (ML) receiver. In this case the ML receiver consists in a continuous-time filter matched to the transmitted pulse shape, followed by a sampler and a threshold detector. When using OOK with duty cycle $0 < \gamma < 1$ the bandwidth requirement increments by a factor $1/\gamma$, however this increment provides a decrease of the average optical power necessary to meet the BER target (usually 10^{-6} for diffuse systems); the reason is that the increased noise associated to this expanded bandwidth is outweighed by the $1/\gamma$ increase in peak optical power. Thus, OOK with RZ is usually preferred to NRZ in infrared systems.

PPM Pulse Position Modulation is an orthogonal modulation scheme that offers a decrease in the average-power requirement compared to OOK, at the expense of an increased bandwidth requirement. In particular L-PPM uses symbols consisting of L time slots also referred to as chips. A constant power $L \cdot P_t$ is transmitted within one chip while zero power is transmitted during the remaining $L - 1$ chips, thereby encoding $\log_2 L$ bits. For a given bit rate, LPPM requires more bandwidth than OOK by a factor $\frac{L}{\log_2 L}$, (e.g., 16PPM requires four times more bandwidth than OOK), but PPM can achieve much greater immunity to neardc noise from fluorescent lamps than OOK. In the absence of multipath distortion, L-PPM yields an average-power requirement that decreases steadily with increasing L; this average power reduction makes PPM especially suitable for portable devices. On the other hand, PPM presents two drawbacks: increased transmitter peakpower requirement, and the need for both chip and symbol level synchronization. In the absence of multipath distortion, an optimum ML receiver is a continuous-time matched filter matched to one chip, whose output is sampled at chip rate. Each block of L samples is passed to the decoder that can be an hard-decision or a soft-decision decoder yielding $\log_2 L$ information bits. The hard decision decoder is characterized by a threshold detector that quantizes to "low" or "high" the samples and the decision

is based on which sample is "high". In the soft decision decoder the samples are unquantized, and the block decoder chooses the largest of L samples.

Subcarrier Modulation In single-subcarrier modulation (SSM) a bitstream is modulated onto a radio-frequency subcarrier, and this modulated subcarrier is modulated onto $X(t)$, the instantaneous power of the infrared transmitter. Provided that the optical signal must be non negative, a dc bias must be added if the subcarrier is a sinusoid. The transmitted waveforms and PSD of a BPSK subcarrier are shown in Figure 1.12(d) and 1.13, respectively, assuming a subcarrier frequency equal to the bit rate. The required bandwidth of such a BPSK subcarrier is twice the bandwidth of an OOK signal, while a QPSK subcarrier requires the same bandwidth as OOK. After optical-to-electrical conversion at the receiver, the subcarrier can be demodulated and detected using a standard BPSK or QPSK receiver.

Multiple access strategies and Optical Orthogonal Codes (OOC) In optical wireless communications MA schemes are mainly based on Time Division Multiple Access (TDMA) and Code Division Multiple Access (CDMA). In TDMA each user is allowed to transmit only within a specified time interval (Time Slot). Different users transmit in different Time Slots. With TDMA separation between users is performed in the time domain, thus each transmitting user can use the whole available frequency bandwidth. TDMA access technique can be use if the network infrastructure is centralized with a coordinator node because it is necessary for the coordinator to send to all nodes periodic reference burst aimed at defining the time frames in which user can transmit. In real communications there are significant delays between users, thus burst references are received with different phases from this reasoning guard times inside time slots are necessary. Moreover since each traffic

burst is transmitted independently with an uncertain phase relative to the reference burst, there is a need for a preamble at the beginning of each traffic burst. This preamble allows the receiver to estimate time and carrier phase. In CDMA techniques each user has assigned a different code (with uncorrelation properties) used to encode data. Thus, different user can transmit in the same time, exploiting the whole available system bandwidth. Codes used in CDMA are called spreading codes due to their particularity of spreading the bandwidth of the encoded signals, in fact CDMA is based on spread-spectrum modulation. Tanks to the uncorrelation property of the codes receiver can ideally perfectly recover the received signal knowing the transmitter code. However transmissions of different users of the networks are not synchronized and this cause a partial loss of the uncorrelation of codes, that become partially correlated. Partial correlation cannot be totally canceled but can be mitigated by proper choice of the spreading codes. CDMA Channel capacity is limited by the number if other users rather than by thermal noise. Furthermore, in CDMA systems is necessary to perform a power control of the power level of the transmitters, because a typical problem to deal with is near-far problem present whenever all users transmit at the same power level (the received power is higher for transmitters closer to the receiving antenna). An optical orthogonal code is a family of (0,1) sequences with good auto- and cross-correlation properties [13],[14], [15], [16]. OOC has thumbtack-shaped auto-correlation that enables the effective detection of the desired signal, and low-profiled cross-correlation make it easy to reduce interference due to other users and channel noise. An OOC family is composed by unipolar sequences suitable for OOK modulation. In general an $(n,w,\lambda_a,\lambda_c)$ OOC is a family of binary sequences of length n and weight w, with unipolar auto-correlation and cross-correlation constraints λ_a and λ_c, respectively:

$$\sum_{t=0}^{n-1} x_t x_{t+\tau} \leq \lambda_a \tag{1.3}$$

$$\sum_{t=0}^{n-1} y_t x_{t+\tau} \leq \lambda_c \tag{1.4}$$

for any $x \neq y \in C$ and any integer t. Aimed at reducing the correlation between different codes, the maximum cross correlation between any two different code sequences should be zero. However, real binary (0,1) sequences, that is sequences for truly positive systems, such as optical systems, can not achieve a cross-correlation value 0, as the coincidences do not cancel out unlike in (+1,-1) sequences. Hence, the minimum possible value of cross-correlation is 1. An (n,w,λ_a,λ_c) OOC C can be alternatively considered as a family of w sets of integers modulo n in which each w set corresponds to a codeword and the integers within each w set specify the nonzero bits positions of the codeword. For instance, the simple OOC 1101000 is referred by (7,3,1,1) but also {0,1,3}(mod 7). Then the auto-correlation and cross-correlation properties can be reformulated, respectively as reported in [15]:

$$|(a + X) \cap (b + X)| \leq \lambda_a \tag{1.5}$$

for $X \in C$ and any $a \neq b$ mod(n), and

$$|(a + X) \cap (b + Y)| \leq \lambda_a \tag{1.6}$$

for any $X \neq Y \in C$ and any a,b. Here $a + X$=$\{a + x : x \in X\}$ and all integers under consideration are taken modulo n. In Figure 1.14 (a) and (b) two different codewords are shown. In (c) and (d) the auto-correlation and the cross-correlation are, respectively depicted. The size of a code C that is $|C|$, denoted by M, is the number of codewords in it. The cyclic shift of a codeword is not considered as another codeword. Provided that is desirable to have OOC with the largest possible number of codewords M, many studies in literature refers to upper and lower bounds for OOC. The largest possible size of an (n,w,λ_a,λ_c) code is denoted by $\Phi(n,w,\lambda_a,\lambda_c)$. A code that has maximum possible size M=$\Phi(n,w,\lambda_a,\lambda_c)$ is said to be an optimal

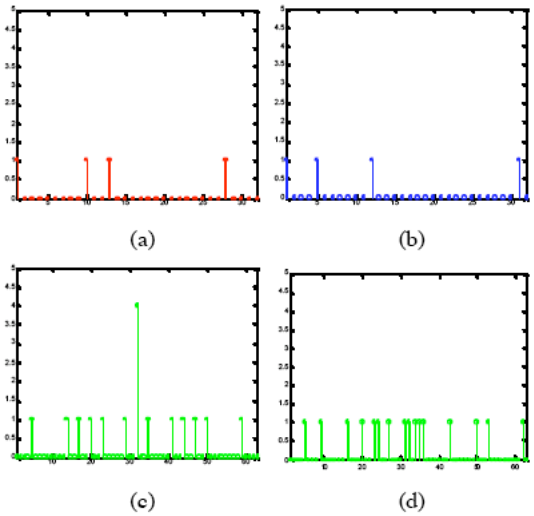

Figure 1.14. (a) and (b) two different OOC codewords belonging to the (32,4,1,1) family, (c) auto-correlation, (d) cross-correlation.

code. There exists many different methods to construct Optical Orthogonal Codes like using Iterative Construction, Projective Geometry [15], but also using Error Correcting Codes [16]. The use of OOC allow optical systems to increment the system capacity in terms of the number of users that are transmitting at the same time. Every information bit is encoded with the OOC and et receiver side correlator-type decoders are used to neglect interfering signals. When the total number of users goes up, the cross-correlation due to interfering users adds up to quickly to severely degrade the system performance. To avoid this phenomenon, both w and n should be increased simultaneously. If we increase only w fixing n, cross-correlation value due to the interference can be lowered because. However, OOC has a very sparse marks to keep the cross-correlations low, i.e. a number of zeros is much higher than that of ones in the sequence. It means that the cross-correlation increases itself by increasing only w. Anyway even increasing both w and n has a drawback, that is a long signal processing time due to long n. After the correlator matched to the single user signal, the receiver has threshold that is used to take decisions on the

correlator output. The threshold Θ value can be chosen under the condition:

$$0 \leq \Theta \leq w \tag{1.7}$$

Two different types of detector can be considered, soft-limiting and hard limiting. The main difference is that in the soft-limiting detector, the contribution of a single tap (the decoder is composed by tapped-delay lines) equals the number of pulses it senses. If there are Θ or more pulses, it outputs 1. In the hard limiting detector, the contribution of a tap is one when it senses one or more pulses and zero otherwise. The detector outputs a 1 when Θ or more taps contribute 0 otherwise. The difference between the two types of detectors is best illustrated when a small number of taps on a single delay line are sensing a number of pulses. The soft-limiting detector will produce a 1, while the hard-limiting type will not. Error probabilities for both different correlator can be found in [15] and [14].

Optical Orthogonal Codes will be used in in this work for system simulation aimed at achieving a performance improvement as it will described in 3.2 and subsequently shown by simulation results. As regards resource management and control (Medium Access Control (MAC)), Carrier-Sense Multiple Access by Collision Avoidance (CSMA-CA) strategies are the most commonly adopted in commercial systems. By these strategies, a transmitter senses the channel and avoids transmitting when hearing the channel as busy. Other methods such as the well-known Carrier-Sense Multiple Access by Collision Detection (CSMA-CD) are difficult to use in the optical context for similar problems to those experienced in RF wireless; typically a transmitter that is actively transmitting is not able to detect another transmission that is to detect a collision. The Advanced Infrared (AIr) Medium Access protocol used by Irda will be further presented (1.3).

1.2.1 Optical Emitters

Two are the processes by which a source can emit light: *spontaneous emission* where an electron makes a transition from a high energy state E_2 to a lower energy state E_1 resulting in the emission of a photon, and *stimulated emission* where a photon, with an energy equal to $(E_2 - E_1)$, interacts with an atom in the upper energy state, causing it to return to the lower state and emit thus a second photon with same phase, frequency, and polarization as the first. Semiconductor sources are based on p-n junctions, and we will consider two different light emitter types: the Light Emitting Diode (LED) that produces scattered incoherent light and is electrically simple to use and control, and the Light Amplification by Stimulated Emission of Radiation (LASER) diode that produces a narrow beam of coherent light and requires a more complex control than a LED.

Light Emitting Diodes (LEDs) produce light following the spontaneous emission principle, while stimulated emission is the basic principle of operation of Light Amplification by Stimulated Emission of Radiation (LASER) based-devices that is laser diodes. Basic properties of laser light are [17]:

- **Monochromaticity** This property is related to wavelength and thus colour. A wavelength specifies the colour at which the laser lases. Ordinary coloured light consists of a broad range of wavelengths covering a particular portion of the visible-light spectrum. Laser beams consist of an extremely narrow range of wavelengths, is thus common to refer to red, green, or blue lasers (but not white laser). Laser beams are said to be nearly "monochromatic," or nearly "single-coloured." Near-monochromaticity is a unique property of laser light, meaning that it consists of light of almost a single wavelength. Perfectly monochromatic light cannot be produced even by a laser, but laser light is many times more monochromatic than the light from any other source.

In some applications, special techniques are employed to further narrow the range of wavelengths contained in the laser output and, thus, to increase the monochromaticity.

- **Intensity** This property refers to the intensity of light. The energy emitted by a laser in the narrow spectral region (colour) in which the laser lases, far exceeds that of the sun or of any other known light source!

- **Directionality and Coherence** Common light sources, such as flashlights, light bulbs, or the sun, emit energy in all directions. Devices such as automobile headlights and spotlights contain optical systems that collimate the emitted light, such that it leaves the device in a directional beam; however, the beam produced always diverges (spreads) more rapidly than the beam generated by a laser. A laser, on the contrary, only emits light and only in a very well defined direction. Moreover, common light sources emit light with a random phase. In contrast, lasers emit light at only one phase, according to the coherence property described in the previous section, that is all produced photons are in phase (phase coherence), have the same wavelength (frequency coherence or monochromaticity), and travel in the same direction (spatial coherence).

LEDs are inexpensive and can support input signals with bandwidths up to 100 MHz. Laser Diodes (LDs) produce a narrow beam of coherent light but they require more complex control and are more expensive than LEDs. A LD can support input signals with bandwidths up to tens of GHz and can provide higher optical power outputs than LEDs. Different materials are used to manufacture lasers at 680, 800, 1300, and 1500 nm but the wavelength band between about 780 and 950 nm is presently the best choice for most applications of infrared wireless links, due to the availability of low-cost LEDs and LDs, and because is coincides with the peak

responsivity of inexpensive, low-capacitance silicon photodiodes. The primary drawback of radiation in this band relates to eye safety: it can pass through the human cornea and be focused by the lens onto the retina, where it can potentially induce thermal damage, that is energy is absorbed by the tissue in the form of heat which can cause localized, intense heating of sensitive tissues. The Human responsivity as function of the wavelength is opaque beyond 1400 nm, unfortunately photodiodes presents at this bands are much more expensive and has higher capacitance per unit area than other more common LEDs.

Light emitted by a LEDs follows the spontaneous emission principle. LEDs are simply biased p-n junctions crossed by a forward current. On the p side of the junction empty electron states are occupied by injected electrons from the n side; on the n side empty hole states are occupied by injected holes from the p side. This increased concentration of minority carriers in the opposite type region leads to recombination across the bandgap, releasing energy. This recombination can be non-radiative (dissipated as heat) or radiative, resulting in a photon of energy E_g. Generated photons are radiated in all directions with a wide wavelength range.

Table 1.2. Comparison between LEDs and LDs.

Characteristic	LEDs	LDs
Spectral width	25-100 nm (10-50 THz)	$< 10^{-5}$ to 5 nm ($<$ 1MHz to 2 THz)
Modulation Bandwidth	Tens of kHz to tens of MHz	Tens of kHz to tens of GHz
E/O Conversion efficiency	10-20%	30-70%
Eye Safety	General considered eye-safe	Must be rendered eye-safe, especially for $\lambda < 1400$ nm
Cost	Low	Moderate to high

Different colours LEDs are are available, there are white, blue, green, aqua, red, orange, yellow, violet, ultra-violet, and infrared LEDs. Typical driving current is in the order of mA and the luminous intensity of a LED is measured in Milli Candle Power (mci); this intensity is measured in the most intense portion of the produced beam. Use of LEDs is more common in wireless optical communication than in fiber optics, because coupling sufficient power into a fiber is difficult, thus regarding the communication in fiber, LEDs are restricted to large core fibers. The most common structure of LEDs is the so called Double Heterojunction (DH) or Double Heterostructure. The Heterojunction is an interface between to semicondutcive materials of different bandgap energies (as opposed to a so called homojunction). The p type layer of the p-n junction is a $GaAs$ layer and the n type is a $AlGaAs$

Semiconductor lasers, most important for optical communications, are light emitting diodes with a resonator cavity that is formed either on the surface of the diode or externally. An electric current passing through the diode produces light emission when electrons and holes recombine at the p-n junction in an area called *active area*. The *active area* should be as small as possible in order to confine the laser output and preserve coherence features. Dispersion in the laser output can be reduced by means of special optical filters to produce a good beam shape. The original semiconductor lasers were manufactured from crystals containing a junction between p- and n-type gallium arsenide, but nowadays they use three or four elements from columns III and V of the periodic table (the so-called III-V compounds). Examples of these semiconductors are $Al1\text{-}xGaxAs$ (aluminum gallium arsenide) or $In1\text{-}xGaxAs1\text{-}yPy$ (indium gallium arsenide phosphide). Lasers are used in several applications such as optical-fiber communications, printers or CD players.

Given the quantum efficiency of the diode η, that is the capability of the device in emitting photons, the rate of emitted photons generated by radiative recombination

is:

$$R_p = \eta \frac{i}{q} \tag{1.8}$$

where i is the forward bias current in Ampères and q is the charge on an electron in Coulombs. Each photon has an energy of $h\nu$ Joules, so the optical power P measured in Watts emitted by a LED is given by the product of R_p and $h\nu$:

$$P = R_p \cdot h\nu = \eta \frac{i}{q} \cdot \frac{hc}{\lambda} \tag{1.9}$$

where c is speed of light and λ is the wavelength characterizing the diode. Optical power produced by a LED is thus intrinsically linear with input current and for a given current, output optical power decreases when temperature increases. In Table (1.2) presents a comparison between LEDs and LDs . Typical LEDs emit light into semiangles (at half power) of 10°-30°, thus they are suitable for directed transmission, in non directed systems like Diffuse Wireless Optical systems, multiple LEDs oriented in different directions are employed. In general LEDs cost less and are more safe than LD but they have several drawbacks like typically poor electro-optic power conversion efficiencies of 10-20% (against 30-70% of LDs) and broader spectral widths, which require the use of a wide receiver optical passband, leading to poor rejection of ambient light. The eye safety of infrared transmitters is governed by International Electrotechnical Commission (IEC) standards [49]. It is desirable for infrared transmitters to conform to the IEC Class 1 allowable exposure limit (AEL), implying that they are safe under all foreseen circumstances of use, and require no warning labels. At pulse repetition rates higher than about 24 kHz, compliance with this AEL can be calculated on the basis of average emitted optical power alone. The AEL depends on the wavelength, diameter, and emission semiangle of the source. At present, the IEC is in the midst of revising the standards applying to infrared transmitters. Based on proposed revisions, at 875 nm, an IrDA-compliant source having an emission semiangle of 15° and diameter of 1 mm can emit an average

power up to 28 mW. At the same wavelength, a Lambertian source (60° semiangle) having a diameter of 1 mm can emit up to 280 mW; at larger diameters, the allowable power increases as the square of the diameter.

1.2.2 The real optical channel

Optical channels fall into three main categories: guided channels, corresponding to fiber optics, unguided but directed transmission (also called Line-Of-Sight or LOS) typical of outdoor optical channels, and, finally, indoor diffuse channels where transmission between mobile terminals is made possible thanks to bounces on the reflecting surfaces of obstacles (e.g. ceilings, walls, furniture, windows). We will now introduce fiber optics basics before describing Free Space Communication (FSO) systems and Diffuse Wireless Optical (DWO) systems.

Optical Fibers

The optical fiber can be defined a cylindrical dielectric waveguide made of low-loss materials such as silica glass, guiding light injected by either a LED or a laser at one end throughout the other end [18]. The fiber consists in a core, in which the light is held, and a cladding that surrounds the core see Figure(1.15). Light confinement in the core is obtained thanks to total-internal refection; since the cladding has a lower refractive index than the core, light rays reflect back into the core when they encounter the cladding at a shallow angle, smaller than a critical angle. When that critical angle is exceeded a ray may even escape from the fiber. Fibers can be classified according to propagation properties and in particular one can find:

Multimode fibers These have a typical diameter in the 50-to-100 micron range for the light carry component. As a result, some of the light rays that make up the digital pulse may travel a direct route, whereas others zigzag as they bounce off

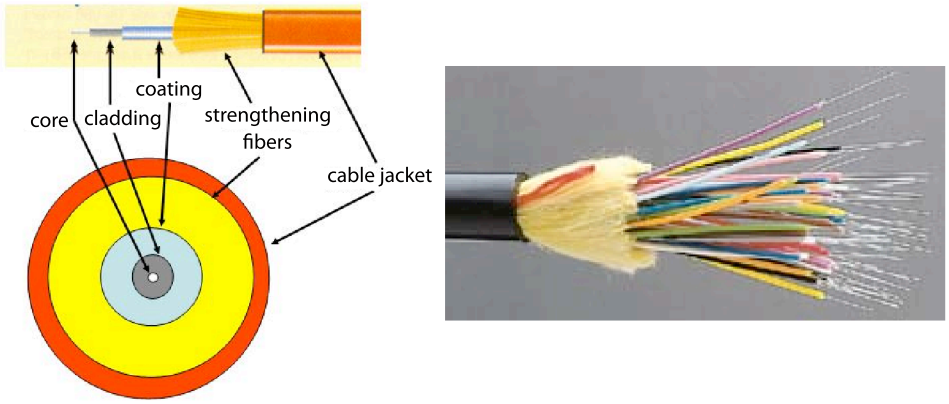

Figure 1.15. Section diagram of an optical fiber (left) and a bunch of fibers (right).

the cladding. These alternative pathways cause the different groupings of light rays, referred to as modes, to arrive separately at a receiving point. The pulse, an aggregate of different modes, suffers from dispersion that is it spreads out and looses its well-defined shape. Multimode fibers can support relatively high transmission rates but over relatively short distances (about 1 km). For larger distances, transmission rates are fairly limited.

Monomode optical or single-mode fibers These are single stands of glass fibers with a very narrow core diameter that allows only one mode of transmission. Although at a larger cost, monomode fibers can carry much higher transmission rates at 50 times the distance compared to multimode fibers, but require light emitters with narrow spectral width.

Multimode fibers that have larger diameter than monomode fibers are also characterized by how reflection occurs within the core. A typical problem of multimode fibers is an effect called modal dispersion, that arises from the differences among the group velocities of the modes inside the fiber. This effect limits the rate at which two different pulses can be sent without overlapping in time and therefore the speed

at which a fiber-optic communication can operate [19]. Modal dispersion can be reduced by grading the refractive index of the fiber core from a maximum value at its center to a minimum value at the core-cladding boundary. The fiber is then called a graded-index fiber, whereas conventional fibers with constant refractive indices in the core and the cladding are called step-index fibers. Old generation fibers were step-index multimode Fibers with a large core measuring up to 100 microns in diameter. The time interval between pulses needed to be large in order to mitigate at the receiver inter-pulse interference provoked by pulse dispersion. As a consequence, the available bandwidth was limited and transmission covered rather short distances (as in an endoscope). In Graded-Index Multimode Fibers the core is characterized by a refractive index that gradually diminishes from the center axis out towards the cladding. Due to the higher refractive index at the center, light rays travelling along the center axis have a lower propagation speed than those moving near the cladding. Also, rather than zigzagging off the cladding, light in the core curves helically because of the graded index, reducing its travel distance. The shortened path and higher speed allow light at the periphery to arrive at a receiver at about the same time as the slow but straight rays along the core axis. As a result pulse dispersion is reduced.

The most important feature of fiber optics is its immunity to electrical interference. *Fibers convey pure optical signals.* They are non conductive media and no electricity runs through them. Therefore, signals travelling over different fibers do not interfere with one another and with electrical equipment. Additional benefits of fiber optics are security since the signal is confined in the core and there are no emissions of electromagnetic energy, and the compact size.

FSO

In FSO, the most common communication medium is the air [20]. The communication link is formed by two highly accurately aligned optical transceivers (see Figure 1.5). Each transceiver pair includes one receiver (visually distinguished as the largest lens on the device) and one or more transmitters. A feasible use of an FSO system is the installation of the "last mile" link from the fiber backbone directly to the client or between different buildings [4]. FSO system performance is primarily dependent upon the climatology and physical characteristics of the installation location. Atmospheric turbulence degrades performance of free-space optical links, particularly over ranges of the order of 1 km or more [21],[3]. Atmospheric turbulence provokes discontinuities in the temperature and pressure of the atmosphere that lead to variations in the refractive index along the link that will cause fluctuations in both the intensity and phase of the received signal and lead to an increased link error probability. In Fig 1.16 is shown the bandwidth demand of a FSO system, and the potential distances covered by the link. The statistical analysis

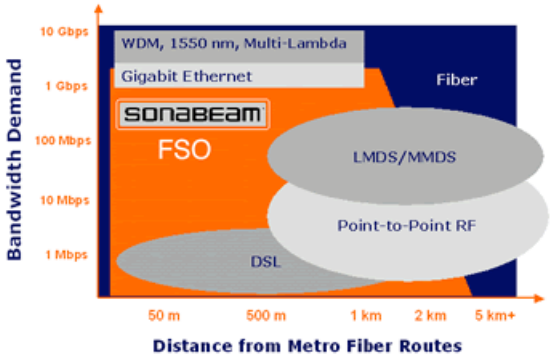

Figure 1.16. FSO system bandwidth demand vs covered distances.

of turbulence-induced losses is used to determine the *Burst Error Probability* (BEP) of the system that can be considered as a Quality of Link (QoL) measure. BEP is

defined in terms of the probability density function of attenuation and is the sum of three effects: beam wander, incidency angle fluctuations, and scintillation. Another limiting factor for BEP is aerosol scattering. Although rain and snow can hamper light propagation, the most detrimental environmental conditions for urban FSO are fog and haze, due to their high concentration of scattering particles with radii on the same order of magnitude as laser wavelengths. Scattering is the deflection of incident light from its initial direction, which causes spatial, angular, and temporal spread, and results in attenuation and distortion of the transmitted signal (on the order of tens to even hundreds of dB/km), and may drive to the loss of the link.

In general, the scattering phenomenon depends upon the ratio x between particle size r to radiation wavelength λ, according to the following equation:

$$x = \frac{2 \cdot \pi \cdot r}{\lambda} \tag{1.10}$$

When the ratio defined in the above equation is much larger than 1 that is when particle size r is much larger that radiation wavelength λ, as in raindrops and snowflakes for example, particles do not seriously impede light propagation. Oppositely, particles that are much smaller than λ introduce scattering of the incident waves named as *Rayleigh scattering*. This phenomenon produces deviations of light particles and attenuate incident power according to the 4^{th} power-law of the wavelength. The worst condition which in fact corresponds to the presence of aerosols is when ratio r is close to unity and as a consequence scattering is determined by the *Mie solution* to the Maxwell wave equation.

In summary, the FSO channel is characterized by three parameters: maximum BER, maximum atmospherical attenuation used to determine the lost-link condition as a function of local atmospheric conditions, and the BEP as a measure of link degradation due to turbulences.

Diffuse Wireless Optical Channel

Wireless optical diffuse communications are typically used in short-range indoor channels (1 to 5 meters). They are usually based on infrared radiation since visible light is seriously affected by artificial illumination. That region of the electromagnetic spectrum offers a virtually unlimited bandwidth that is unregulated worldwide. As they are designed for indoor scenarios, these systems are strictly limited by safety regulations, leading to use of infrared LEDs rather than lasers. Infrared radiation exhibits qualitatively similar behaviour to visible light. Both are absorbed by dark objects, diffusely reflected by light-coloured objects, and directionally reflected from shiny surfaces. Both penetrate through glass, but not through walls or other opaque barriers, so that infrared transmissions are confined to the room in which they originate. This confinement makes it easy to secure transmissions against casual eavesdropping, and it prevents interference between links operating in different rooms.

Diffuse transmitters radiate optical power over a wide solid angle in order to ease the pointing and shadowing problems of point-to-point links[22]. This transmission technique exploit the fact that a wide variety of common buildings materials are efficient diffuse infrared reflectors. An example of optical diffuse system is shown in Figure(1.17).The transmission is a non directed NLOS, that is the transmitter does not need to be aimed at the receiver since the radiant optical power is assumed to reflect from the surfaces of the room. Thus, users of a diffuse optical system have a wide degree of mobility at the expense of a high path loss. A model for the optical Path Loss (PL) can be found in [23] and the behaviour of the received optical power (normalized with the channel gain) is shown in Figure(1.18). As further described, we will use this model in some of our system simulations. Unlike radio frequency wireless channels diffuse channels do not exhibit fading. This is due to the fact that

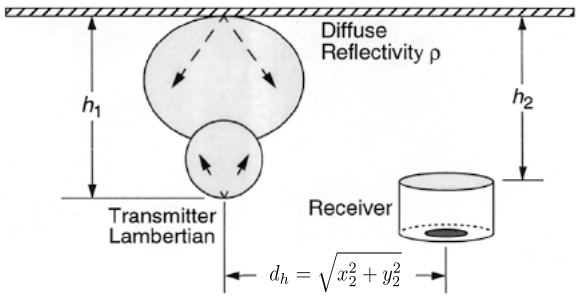

Figure 1.17. Example of diffuse optical system.

the receive photodiode integrates the optical intensity field over an area of millions of square wavelengths and hence no change in the channel response is noted if the photodiode is moved a distance on the order of a wavelength. Thus the large size of the photodiode relative to the wavelength of light provides a degree of spatial diversity which eliminates multipath fading. Many channel models based on measurements allow for the accurate simulation of the impulse response of the channel [24]. Optical indoor channels can be modelled with similar techniques as RF indoor channels. Besides iterative and statistical approaches, the most proper technique seems to be ray-tracing combined with models for reflecting surfaces.

Consider a non directed NLOS infrared channel using intensity modulation and direct detection.As it will shown in the receiver description, the input signal $X(t)$ is the instantaneous optical power of the emitter, and the output of the channel $Y(t)$ is the instantaneous current in the receiving photodetector, which is the product of the photodetector responsivity ρ and the integral over the photodetector surface of the instantaneous optical power at each location. The signal propagates within a room whose surfaces (e.g. walls, ceiling,..) has reflectivity properties. In the

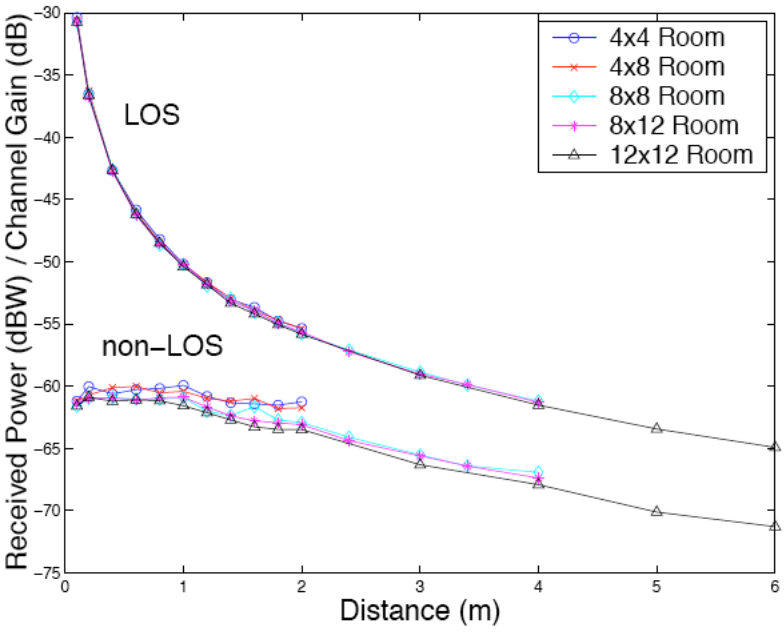

Figure 1.18. Path Loss of an indoor optical system for both LOS and NLOS cases.

presence of intense infrared and visible background light, which results in additive, white, nearly Gaussian shot noise $n(t)$ the channel can be modeled as a baseband system like:

$$Y(t) = \rho X(t) \otimes h(t) + n(t) \tag{1.11}$$

where $\otimes$ denotes the convolution. The channel impulse response of this system is different from the one characterizing the radio environment because here the reflection of infrared radiation (and, indeed, visible light) by most surfaces in typical rooms is predominantly diffuse, i.e., the reflected light is scattered into a continuous distribution of angles, which is nearly independent of the incident angle. Hence,when a reflecting object is illuminated by the transmitter and this object lies in the receiver field of view, the result is a pulse extended in time . The temporal dispersion of $h(t)$ can be expressed by the *channel rms delay spread* D or by its normalized version

D_{T_b} that is D/T_b where T_b is the bit duration. According to [24] the channel impulse response of the LOS channel can be modeled with an exponential decay function, that is the channel impulse response can be modeled as a sequence of delta functions whose amplitudes decay geometrically. For the diffuse NLOS channel, the impulse response can be evaluated with a model called *ceiling bounce model* according to which, if some reasonable hypothesis are made (the ceiling is approximated as an infinite Lambertian-reflecting plane and the transmitter/receiver couple both facing up has the same distance from the ceiling) can be expressed by:

$$h(t) = \frac{\overline{\rho}A}{3\pi H^2}\frac{6(2H/c)^6}{(t+2H/c)^7}u(t) \tag{1.12}$$

where $\overline{\rho}$ is the surface reflectivity, A is the receiver area H is the height of the ceiling above the transmitter and receiver, c is the lightspeed and $u(t)$ is the Heaviside's unit function. It we call $G_0 = \frac{\overline{\rho}A}{3\pi H^2}$, $a = 2H/c$ and assume $G_0 = 1$, we can rearrange the impulse response the *ceiling bounce model impulse response*:

$$h_c(t,a) = \frac{6a^6}{(t+a)^7}u(t) \tag{1.13}$$

the delay spread for the ceiling bounce model can be expressed by:

$$D(h_c(t),a) = \frac{a}{12}\sqrt{\frac{13}{11}} \tag{1.14}$$

Multipath distortion tends to make the non-directed diffuse channel low-pass frequency giving the rise to a channel bandwidth limit of approximately 10-200 MHz depending on room layout shadowing and link configuration. High frequency components suffer multipath distortion more. Even if the diffuse channel is characterized by multiple reflections, other contributions after the first bounce has low impact, thus the *ceiling bounce model* well model the ISI impact due to multipath distortion. Usually rectangular pulses are used transmitted in air, as it is remarked by [25], different pulse shapes like squared sine or the offset cosine yields better performance due to a lower inter symbol interference. The *ceiling bounce model* will be used in our system simulations as it will further described in section (3.1).

Ambient Light Noises

The most commonly encountered ambient light sources are sunlight, skylight, incandescent and fluorescent lamps [26],[6],[1]. The optical spectral power densities of some of them are shown in Figure (1.19). As shown, the spectrum produced by an electronic-ballast driven fluorescent lamp consists of low and high frequency regions; the low frequency region resembles the spectrum of a conventional fluorescent lamp while the high frequency region is attributable to the electronic ballast. In addition artificial sources emit rapidly fluctuating components associated with higher harmonics of the mains frequency. These components can reduced by electrical filtering. A deterministic expression that models the interfering signal at the output

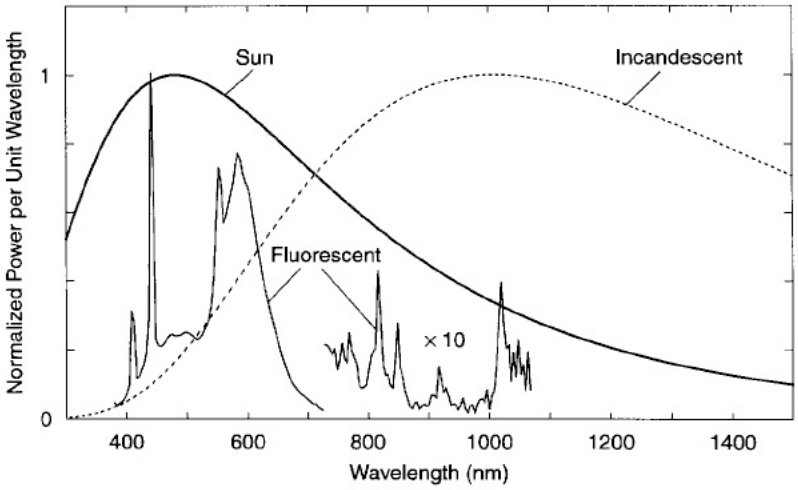

Figure 1.19. Optical spectra of common ambient infrared sources scaled to have the same maximum value.

of the photodiode is in [26]. Noise sources can be organized into these categories:

- Sunlight irradiance produces shot noise in the photodiode that can be considered as a white Gaussian noise. This noise can be reduced by using tinted lenses that avoid visible and UV spectral components. Solar irradiation (also

called insolation) arrives at Earth at wavelengths determined by the photospheric temperature of the sun (peaking near 5600 °C). The main wavelength interval is between 200 and 3400 nm (0.2 and 3.4 μm), with a maximum power input close to 480 nm (0.48 μm).

- Artificial lamps (incandescent, halogen and fluorescent) produce shot noise in the photodiode that can be considered as a narrowband interference. The effect of incandescent or halogen lamps can be seen as a near-dc photocurrent. On the other hand, fluorescent lamps (especially when driven by electronic ballast) emit an infrared signal that is periodically modulated at rates of tens of kHz, and which can severely impair the performance of IR wireless links. Fluorescent lamps emit strongly at spectral lines of mercury and argon that lie in the 780-950 nm band of interest for low-cost infrared systems. This effect can be reduced by means of lenses and optical filtering (similar to a bandpass filter, but designed based on wavelength rather than frequency), or also by coding and modulation, for example adopting spread spectrum modulation the artificial light interference behaves like a narrow band jammer, hence its effect reduced thanks to the processing gain advantage of the spread spectrum technique.

- Thermal noise at receiver has similar nature of any electronic device and is modelled by the Boltzmann equation.

- Dark current that is a spurious current level produced in the photodiode.

Part of the incident ambient light can blocked by optical filers with a passband corresponding to the transmitting LED bandwidth, different filters "absorption edge filters" block only the visible part of the spectrum. A type of filters that is used in almost all present commercial infrared systems is the "longpass filter", this can be thought as a filter that allow to pass all the wavelength beyond wavelength and

are independent of the angle of incidence. The use of longpass filters combined with silicon p-i-n diodes exhibits a bandpass optical response since the silicon device does not respond to wavelengths beyond about 1100 nm. In the particular case of indoor optical communications the interference produced by fluorescent lamps driven by electronic ballasts causes very large power penalties and the entire ambient light level varies over several orders of magnitude. Bandpass filters are usually constructed of multiple thin dielectric layers, these filters can achieve narrow bandwidths, leading to superior ambient light rejection (bandwidths below 1 nm are available commercially).

1.2.3 Optical Receivers

Optical receivers are transducers capable of transforming optical signals into electrical signals and are called photodetectors. Photodetectors can be classified as Photodiodes, Phototransistors Photoconductive devices and Photomultiplier tubes.

Photodiodes By far the most common photodetector, a photodiode is a p-n junction designed to be responsive to optical input.

Phototransistors These are bipolar transistors encased in a transparent case so that light can reach the Base-Collector diode. The phototransistor works like a photodiode, but with a much higher sensitivity to light, because the electrons that tunnel through the Base-Collector diode are amplified by the transistor function. They are more sensitive than photodiodes but, as their temporal response is much slower than in a photodiode, their not usually used in optical communications.

Photoconductive devices and Photomultiplier tubes These are high-sensitivity devices that are far more expensive than photodiodes and phototransistors. They

require high bias voltages that make them not practical for optical communications.

The availability of low-cost, low capacitance, large area silicon photodiodes working in the band of low-cost LED transmitters (that is approximately 780-950nm), made this reliable optical element used receiver almost in all optical communication systems. Photodiodes can be used in either zero bias or reverse bias. In zero bias, light falling on the diode causes a voltage to develop across the device, leading to a current in the forward bias direction. This is called the *photovoltaic effect*, and is the basis for the operation of solar cells (in fact a solar cell can be considered as a large number of big, cheap photodiodes). Diodes usually have extremely high resistance when reverse biased. This resistance is reduced when light of an appropriate frequency shines on the junction. Hence, a reverse biased diode can be used as a detector by monitoring the current running through it. The most attractive characteristics of a photodiode can be summarized as follows:

- High sensitivity at the operating wavelength range (780-950 nm but also 1200-1600 nm)
- Short response time
- Linearity over a wide range
- Stability with respect to time and temperature
- Low cost and high reliability

Two types of silicon photodiodes are widely available on the market: Ordinary silicon "positive-intrinsic-negative" (PINs) photodiodes and "avalanche photodiodes" (APDs). PINs are at present extensively employed in nearly all commercial infrared links. APDs are essentially p-i-n devices, but operated at a very high reverse bias, so that photogenerated carriers create secondary carriers by impact ionization,

resulting in internal electrical gain. In principle, this internal gain helps to overcome receiver amplifier thermal noise, by increasing the receiver SNR when other sources of noise, that is ambient noise, is weak. When ambient noise is dominant, however, the random nature of the APD's internal gain reflects in an increase in the variance of the shot noise, and as a result the SNR decreases. Other drawbacks are a higher cost compared to PINs, and temperature-dependent gains. Since our scope is the simulation of a low-cost system, we will restrict the remaining discussion to ordinary PINs.

When an incident instantaneous optical power $p(t)$ reach the photodiode surface, a current is produced in output. This current is called *photocurrent*and it follows the expression

$$i(t) = \rho \cdot p(t) \tag{1.15}$$

where ρ is the responsivity and its unit is (A/W). For a typical silicon photodiode ρ presents a peak about 950 nm. This responsivity can be estimated from another parameter: the *Quantum Efficiency* (Q.E.) η, that is a percentage expressing the photodiode's capability to convert light energy to electrical energy. It depends on the responsivity of the photodiode. Operating under ideal conditions of reflectance, crystal structure and internal resistance, a high quality silicon photodiode of optimum design would be capable of approaching a Q.E. of 80%.

The *risetime* of a photodiode it is referred as (tr) and it is the measure of the photodiode response speed to a stepped light input signal. It is the time required for the photodiode to increase its output from 10% to 90% of final output level. Unless a photodiode should be biased on inverse voltage, when applying an excessive reverse voltage to photodiodes may cause breakdown and severe degradation of device performance. Thus every photodiode is characterized by a *Maximum Reverse*

Voltage referred as (Vr). Any reverse voltage applied must be kept lower than the maximum rated vale, ($Vrmax$). The photodiode's *Linearity* measures the degree of linearity of the photodiodes output. Generally, when reverse-biased, output is extremely linear with respect to the illuminance applied to the photodiode junction. One important parameters of a photodiode is its *Junction capacitance* that depends on its area and the bias voltage. This capacitance limits the bandwidth response of the device, so, unless more active area is needed in order to increase the received optical power, it penalizes the bandwidth response.

An infrared receiver detects an optical power that is proportional to its effective light-collection area. Increasing the photodiode area is expensive, and tends to decrease receiver bandwidth and increase receiver noise. Hence, to increase the effective area of the receiver *optical concentrators* can be deployed. Concentrators may be of the imaging or non-imaging variety. An example of an imaging concentrator is the telescopes used in long-range, free-space optical links. In the short range optical communications, non imaging concentrators are chosen.

The effective area of a receiver depends on the angle of incidence of the incoming ray ψ. If we ignore the reflection losses and consider a photodiode with physical receiving area A using a concentrator covered with a filter, we have [1]:

$$A_{eff}(\psi) = \begin{cases} AT_s(\psi)g(\psi)\cos\psi, & 0 \leq \psi \leq \Psi_c \\ 0, & \theta > \Psi_c \end{cases}$$

where $T_s(\psi)$ is the signal transmission of the filter (if the source bandwidth is not narrow this can be considered an average of the filter transmission over different wavelengths and/or over different angles of incidence if different ray strike are present), $g(\psi)$ is the concentrator gain, Ψ_c is the concentrator FOV (semiangle). Usually $\Psi_c \leq \pi/2$. Non imaging concentrators exhibit a trade-off between gain and FOV. In the particular case of non direct optical communication, hemispherical lens are the most suitable due to the very large FOV ($\Psi_c \approx \pi/2$ and gain $g(\psi) \approx n^2$).

In Figure(1.20) an example of two different hemispherical concentrators is shown. When a longpass filter is is employed, a planar longpass filter can be placed between the hemisphere and the detector. When bandpass filtering is utilized, it is not desirable to employ a planar filter in the configuration shown in Figure(1.20-a). As ψ, the angle from which rays are received, shifts, so does θ, the angle at which light strikes the filter. This shifts the filter passband, decreasing the filter transmission $T_s(\psi)$ for some ψ. Instead, as shown in Figure(1.20-b), the bandpass filter should be deposited or bonded onto the outer surface of the hemispherical concentrator. In this case rays that reach the detector are incident upon the filter at small values of the angle θ independently of the angle ψ, thus minimizing the shift of the filter passband, and maximizing its transmission. Different types of concentrators that privilege the gain respect to the FOV are suitable for different types of systems.

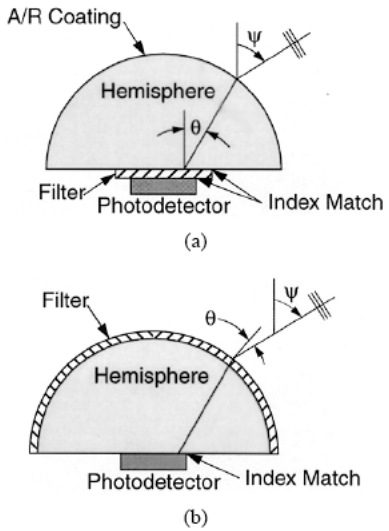

Figure 1.20. Example of two different non-imaging hemispherical optical concentrators: a) with a planar filter and b) with and hemispherical filter.

Receiver Amplifier

After the optical signal has been converted into an electrical signal by the photodetector, it is further processed by the receiver amplifier that also converts the current from the photodiode into a voltage. As in any communication system, the amplifier should introduce as lowest noise as possible onto the received signal. There are typically three ways in which amplification can be accomplished which correspond to the impedance characteristics of the amplification circuit:

- Low impedance (also called a voltage amplifier) producing low thermal noise but lacking bandwidth and as such introducing non-linear distortions. Its scheme is shown in Figure (1.21-a).
- High impedance producing high thermal noise but with reduced non-linear distortions. Given the high gain, this scheme is particularly susceptible to saturations which in turn introduce non-linear distortion which can be mitigated by including a post-front-end equalizer. Its scheme is shown in Figure (1.21-b).
- Transimpedance is, by far, the most common topology. In a transimpedance front-end a feedback resistor is used. The value of this resistor is kept relatively large and thus any current noise contribution is minimized. Its scheme is shown in Figure (1.21-c).

1.3 AIr MAC Protocol

Advanced Infrared (AIr) is a proposed standard of the Infrared Data association (IrDA) for indoor infrared LANs [27]. AIr Medium Access Control (MAC) employs Carrier Sense Multiple Access with Collision Avoidance (CSMA) techniques with

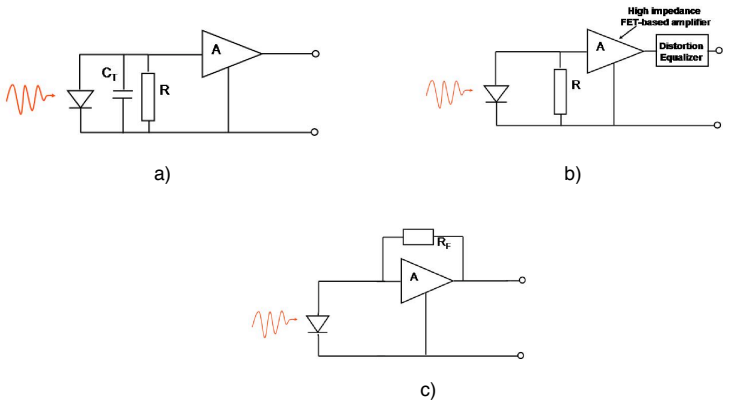

Figure 1.21. a) Low Impedance Amplifier , b) High Impedance Amplifier and c) Trans-Impedance Amplifier.

Request to Send/Clear to Send (RTS/CTS) frame exchange to address the hidden station problem. AIr-MAC sub-layer is responsible for co-ordinating the access to the infrared medium among multiple AIr and IrDa devices. AIr MAC provides Reliable (an acknowledgment is provided for every data packet or every packet burst) and Unreliable (guarantee the transmission of data packets but not the delivery as no ack is provided to indicate correct frame reception) transfer modes and Reserved media access by using the (RTS/CTS). A long collision avoidance Slot time (σ), which includes the beginning of the CTS frame is defined. A station contending for the medium first selects a random number z from a range (0,W-1), where W is the Contention Window (CW). The station waits for z Collision Avoidance Slots (CAS) before transmitting in order to minimise the collision probability. AIr MAC also provides guidelines for linear CW adjustments. For AIr protocol, linear CW adjustment is preferable than the exponential backoff of the similar IEEE 802.11 protocol because the AIr long CAS duration, combined with the high number of empty CAS introduced by the exponential backoff scheme.

Chapter 2

Ultra-wide band communications

2.1 Historical Overview & State of the Art

Ultra-wideband (UWB) is an emerging wireless technology, and has been considered as one of the promising technologies to provide multimedia services in both indoor and outdoor applications.The UWB transmission technique is characterized by an instantaneous spectral occupancy in excess of 500 MHz or fractional bandwidth of more than 20%. With the benefits of high data rate, low power spectral density, capability to capture multipath energy, and ability of accurate positioning, UWB has demonstrated its potential in future multimedia applications as well as in industrial control and maintenance medical monitoring, radar imaging, home automation, etc.

A breakpoint in the history of UWB was when the Federal Communication Commission (FCC) allowed spontaneous UWB indoor and outdoor transmissions between the band from 3.1 to 10.6 GHz on an unlicensed basis [28].

This chapter begins discussing the state-of-the art of UWB and then continues by providing a theoretical framework of UWB radio communications, modulation

techniques and Power Density Spectra. Since this thesis focuses on the convergence between optical and UWB systems, common aspects between this two transmission techniques will be highlighted (i.e pulse signals and pulse based modulations like PPM and OOK.

Despite its renewed interest during the past decade, UWB has a history as long as radio. In Guglielmo Marconi's experiments over a century ago radio communications utilized enormous bandwidth as information was indeed conveyed through a spark-gap transmitter to transmit the Morse Code over the air. Nevertheless technological limitations (spark-gap transmitters were noisy and inefficient) and commercial pressure for more reliable communications strongly favoured, however a shift of research and development towards continuous-wave transmissions. During the World War II pulse transmissions techniques were adopted for security reasons in for military transmissions. Since pulse-based systems were able to guarantee higher ranges compared to continuous transmissions, the former started to be considered also for civilian applications. In fact these systems allowed to regenerate the pulses, thus to avoiding the accumulation of distortion from noise and other system imperfections. Moreover despite being analog, pulse-modulated systems permitted the multiplexing of communication channels on the time division basis. During the 1960s, thanks to high sensitivity to scatters and low power consumption UWB technology was introduced in the radar systems with the works of Harmuth [29], Ross [30] and others [31]. In 1977 the USAF started a research program on IR systems that lasted until 1989. It was in 1989 that the U.S. Department of Defense (DoD) coined the term "ultra wideband" for devices occupying at least 1.5 GHz, or a -20 dB fractional bandwidth exceeding 25% [32].

Modern history of Ultra Wideband starts officially in 2002, when the Federal

Communication Commission (FCC) allowed spontaneous emission of UWB signals among the huge range of frequencies (3.6-10.1GHz) at the noise floor [28]. FCC proposal allowed the coexistence of RF systems and UWB radios, these latter being able to operate using low-power ultra-short information bearing pulses. Since the FCC regulations were released, several research institutions, industry and government agencies undertook efforts to asses and exploit the potential of UWB radios: examples are short-range very high-speed broadband access to the Internet, cable replacement, very accurate (centimeter-level) localization, high resolution ground-penetrating radar, through-wall imaging and many others.

The most common definition of the term Ultra Wideband comes from the UWB radar world and refers to electromagnetic waveforms that are characterized by an instantaneous fractional energy bandwidth greater than about $20-25\%$. UWB signals are very often characterized by the transmission of pulses with a short duration in time (in the order of ns), in this case considering the duration of one pulse, the instantaneous energy must be computed over this interval. However the FCC regulations leave open the possibility of producing UWB signals also with nonimpulsive schemes. In this work however we will focus on Impulse Radio UWB. One source bit can be represented with a single pulse, but commonly a single bit of information involves the processing of several pulses, and in this case the energy bandwidth (that is the energy in the frequency interval $(f_H - f_L)$ is referred to the group of pulses. If more pulses per bit are considered, a well-based definition of useful signal energy must be provided. According to FCC, the Energy Spectral Density (ESD) lower and upper frequencies must be considered at $-10dB$. Thus since fractional bandwidth is defined as $\left(\frac{f_H - f_L}{f_c}\right)$, where f_c is the central frequency, a systems with $f_c \geq 2.5GHz$ need to have a $-10dB$ bandwidth of at least $500MHz$ [33].

If f_L is the lower limit of the Energy Spectral Density (ESD) and f_H is the higher limit, then the center frequency of the spectrum is located at $\left(\frac{f_H+f_L}{2}\right)$ and the fractional bandwidth is defined as the ratio of the energy bandwidth and the center frequency:

$$fb = \left(\frac{f_H - f_L}{\frac{f_H+f_L}{2}}\right) \tag{2.1}$$

For wireless communications the FCC power level regulations are very low (below -41.3 dBm), this power constraint allows UWB to coexist with already available legacy systems such as global positioning system (GPS) and the IEEE 802.11 wireless local area networks (WLANs) within the band 3.6-10.1GHz.

Provided that UWB signal power is forced to be at the noise floor, UWB signals are very difficult to intercept by eavesdroppers and are particularly secure against jamming (AntiJamming capability AJ). These characteristics are typical of spread spectrum schemes that have been recently proposed, for both wireless and wired communications systems, as a way for reducing the effect of jamming and multipath dispersion.

2.2 Principles of Impulse Radio in UWB communications

As previously mentioned the most common and traditional way of emitting an UWB signal is by radiating pulses that are very short in time. This transmission technique goes under the name of Impulse Radio (IR). The way by which the information data symbols modulate the pulses may vary, for example Pulse Position Modulation (PPM), Pulse Amplitude Modulation (PAM) and On Off Keying (OOK) are possible schemes. In addition to modulation and in order to shape the spectrum of the generated signal, the data symbols are encoded using pseudo-random or pseudo-noise

(PN) codes. In a common approach, the encoded data symbols introduce a time dither on generated pulses leading to the so called Time-Hopping UWB (TH-UWB). Direct-Sequence Spread Spectrum (DS-SS), that is amplitude modulation of basic pulses by encoded data symbols, in the IR version indicated as Direct-Sequence UWB (DS-UWB), also seems particularly attractive. RF modulation is rarely mentioned in conjunction with UWB systems, which typically operate in the base-band. While RF modulation is obviously applicable to UWB as well, a shift in operating frequency can be potentially obtained by pulse shaping.

In Figure 2.1 a simple M-ary TH-UWB transmission chain is provided. Given the binary sequence to transmit $\mathbf{b}$=(..,b_0,b_1,..,b_k,b_{k+1},..), generated at a rate of $R_b = \frac{1}{T_b}$ bits/s, a first system repeats each bit N_s times and generates a binary sequence (..,b_0,b_0,..,b_0,b_1,b_1,..,b_1,b_k,b_k,..,b_k,b_{k+1},b_{k+1},..,b_{k+1},..)=(..,a_0,a_1,..,a_j,a_{j+1},..)=$\mathbf{a}$ at the rate $R_{cb} = \frac{N_s}{T_b} = \frac{1}{T_s}$. This system introduces redundancy and is a (N_s,1) block coder indicated as a code repetition coder. In the classical terminology this is a channel coder. A second block called transmission coder applies an integer-valued code $\mathbf{c}$=(..,c_0,c_1,..,c_j,c_{j+1},..) to the binary sequence $\mathbf{a}$ and generates a new sequence $\mathbf{d}$. The generic element of this sequence $\mathbf{d}$ is expressed as follows:

$$d_j = c_j T_c + a_j \epsilon \tag{2.2}$$

where T_c is a time constant that is called "chip time" or "chip distance" and ϵ is the PPM time shift. Since bit time T_b is divided into N_s time slots each with duration of T_s seconds, and each T_s must contain the chip time and the time shift, for all c_j the time constraint $c_j T_c < T_s$ must be provided and this is also true that $\epsilon < T_c$. The code $\mathbf{c}$ is a integer-valued code that can be pseudo-random. If we consider it as a pseudo-random code, its generic element c_j satisfies $0 \leq c_j \leq N_h - 1$ where N_h is the code cardinality. The code $\mathbf{c}$ can be periodic, and in this case, its period is indicated by N_p. In the most commonly adopted case the code period is chosen

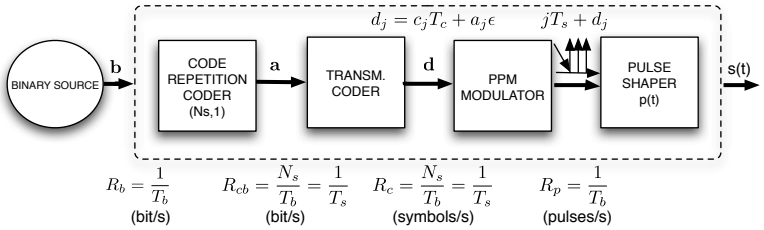

Figure 2.1. Transmission scheme for a PPM-TH-UWB.

equal to the length of the repetition code, this choice has clear effect on the PSD of the transmitted signal [34]. In the presented scheme the transmission coder plays a double role of code division multiple access coder and of spread spectrum shaper of the transmitted signal. The real-valued sequence **d** enters a third system, the PPM modulator, which generates a sequence of unit pulses (Dirac pulses $\delta(t)$) at a rate of $R_p \frac{N_s}{T_b} = \frac{1}{T_s}$ pulses per second. These pulses are located at times $jT_s + d_j$, and therefore shifted in time from nominal positions jT_s by d_j. Pulses occur at times $(jT_s + c_j Tc + a_j \epsilon)$. Note that code **c** introduces a TH shift on the generated signal, and it is for this reason that is indicated as TH code. The shift introduced by the PPM modulator, $a_j \epsilon$, is usually much smaller than the shift introduced by the TH code, $c_j T_c$, that is $a_j \epsilon \leq c_j T_c$, except for $c_j = 0$. The last block in the scheme is the pulse shaper filter with impulse response $p(t)$. The impulse response $p(t)$ must be such that the signal at the output of the pulse shaper filter is a sequence of strictly non-overlapping pulses. The choice of $p(t)$ is crucial since it affects the PSD of the transmitted signal [34]. The TH-UWB transmitted signal can be expressed as follows:

$$s(t) = \sum_{j=-\infty}^{\infty} p(t - jT_s - c_j T_c - a_j \epsilon) \tag{2.3}$$

The generated pulse must be in the order of nanoseconds: this is possible after the introduction of UWB Large Current Radiator (LCR) introduced by Harmuth (1990).

The LCR is current driven, and the antenna radiates a power that is proportional to the square of the derivative of current. When a step function current, for example, is applied to the antenna, a pulse is generated: the steeper the step function current, the narrower the generated pulse. A pulse shape that can be generated in the easiest way by pulse generator has the gaussian shape, and it is described by the following

$$p(t) = \pm\frac{1}{\sqrt{2\pi\sigma^2}}e^{-\left(\frac{t^2}{2\sigma^2}\right)} = \pm\frac{\sqrt{2}}{\alpha}e^{-\left(\frac{2\pi t^2}{\alpha^2}\right)} \tag{2.4}$$

where $\alpha^2 = 4\pi\sigma^2$ is called shape factor and σ^2 is the variance. To be radiated in an efficient way, however, a basic feature of the pulse is to have a zero dc (direct current) offset. Several pulse waveform can be considered, provided that this condition is verified. Gaussian derivatives are suitable, and in particular the second order derivative is the most commonly adopted. In Impulse Radio is possible to shape the spectrum by changing the pulse waveform: basically the spectrum may be shaped in three different ways, i.e. pulse width variations, pulse differentiation and a combination of base functions. The Gaussian pulse used in practice must be truncated to a desired time duration because provided that the pulse is infinite in time ISI between pulses would be unavoidable. In Figure 2.2 is shown an example of a TH-2PPM-UWB transmitted signal. In particular two bits are considered with a repetition coder with length N_s=5.

2.2.1 Power Spectral Density of IR-TH-PPM UWB signal

The Power Spectral Density (PSD) of a TH-PPM UWB signal is reported. Based on the similarities of the signal format 2.3 and the output of an analog PPM modulator consisting of a train of identically shaped and strictly non-overlapping pulses the PSD of a TH-PPM signal was evaluated in [35]. Here the authors show how the PPM signal can be considered modulated by a periodic signal and therefore is reasonable for the PSD to be discrete and have frequency components at the

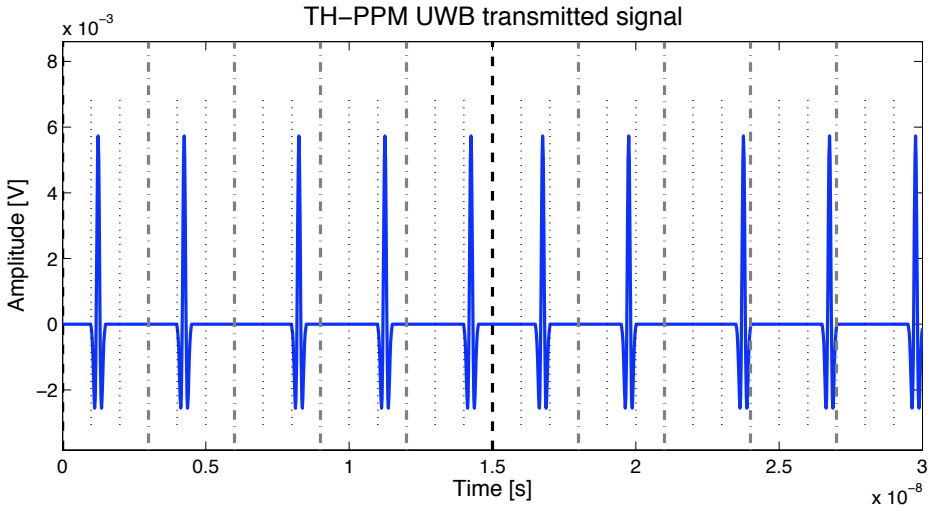

Figure 2.2. Example of UWB TH-PPM transmitted signal with N_s=5, average transmitted power=-30dB, T_s=3ns, T_c=1ns, N_h=3, N_p=5, T_m=0.5ns, α=0.25ns and ϵ=0.5ns.

fundamental. As reported also in [34], the fundamental frequency that influences the PSD shape depends on the period of the code (N_p), that is the fundamental is $f_p = 1/T_p = 1/(N_p T_s)$, where T_s is the pulse interval of the system. Must be noted that the pulse repetition frequency $1/T_s = N_p/T_p$ is a multiple of the fundamental frequency of the periodic waveform; therefore, the PSD is composed of lines occurring at $1/T_b$ and its armonics. If, as common in practice, N_p is set equal to N_s, that is, the periodicity of the code coincides with the number of pulses per bit, spectrum lines occur at $1/T_b$ and its armonics, where $T_b = N_s T_s = N_p T_s$ is the bit interval.

Provided that the source b is a strict-sense stationary discrete random process, and the different extracted variables b_k are statistically independent with a common probability density function w, then the PSD of a TH-PPM UWB signal with $N_p = N_s$ can be expressed by:

$$P_s(f) = \frac{|P_\nu(f)|^2}{T_b}\left[1 - |W(f)|^2 + \frac{|W(f)|^2}{T_b}\sum_{n=-\infty}^{+\infty}\delta\Big(f - \frac{n}{T_b}\Big)\right] \tag{2.5}$$

where $P_\nu(f)$ is the Fourier transform of a signal $\nu(t)$ called "multi-pulse", that is a signal that takes count of all the N_s pulses that are used for the transmission of a single bit. The TH-PPM signal can be imagined as sequence of multi-pulse signal. If we define the single multi-pulse signal as:

$$\nu(t) = \sum_{j=1}^{N_s} p(t - jT_s - \eta_j) \tag{2.6}$$

where η_j is the the time shift due to the TH code, its Fourier transform can be expressed by:

$$P_\nu(f) = P(f) \sum_{m=1}^{N_s} e^{-j(2\pi f(mT_s+\eta_m))} \tag{2.7}$$

The term $|W(f)|^2$ that is the weight value of the spectral lines, depends on the statistical properties of the source. An example of the Power Spectral Density of a TH-PPM UWB signal is shown in Figure(2.3). The provided spectrum shape is

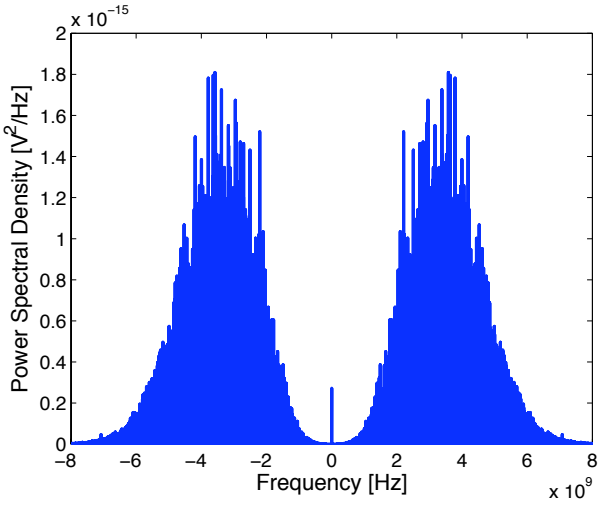

Figure 2.3. PSD of an IR-TH-PPM UWB signal.

strictly dependent on the used TH code: in fact the effect of the code in fact is to whiten the spectrum since power distributes over a larger number of spectrum lines and spectral peaks are less accentuated.

2.2.2 Emission masks

UWB radio signals must coexist with other radio signals. Possible interference from and onto other communications systems must be contained within regulated values that indicate the maximum tolerable power be present in the air interface at any given frequency. For this reason in 2002 FCC released 2 different emission masks. Mainly 3 types of UWB devices were defined, Imaging Systems, Communication and Measurement Systems and Vehicular radar, thus both the outdoor and the indoor channels must be considered. Emission masks impose power limitations on the effective radiated power and differences between outdoor and indoor masks are more stringent power constraints for the outdoor environment in the band between 1.99-3.1GHz and above 10.6GHz. The effective radiated power is the Effective

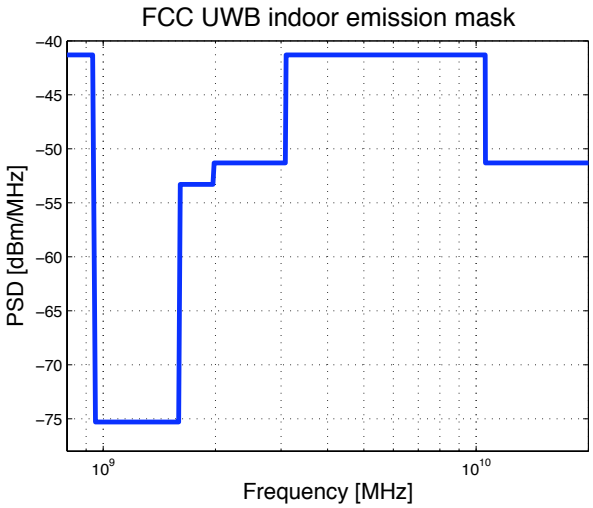

Figure 2.4. FCC indoor emission mask for UWB devices (FCC,2002).

Isotropic Radiated Power (EIRP) for a given range of operating frequencies, and is given by the product of available power of the transmitter P_{TX}, which is the maximum power that the transmitter can transfer to the transmitter antenna and

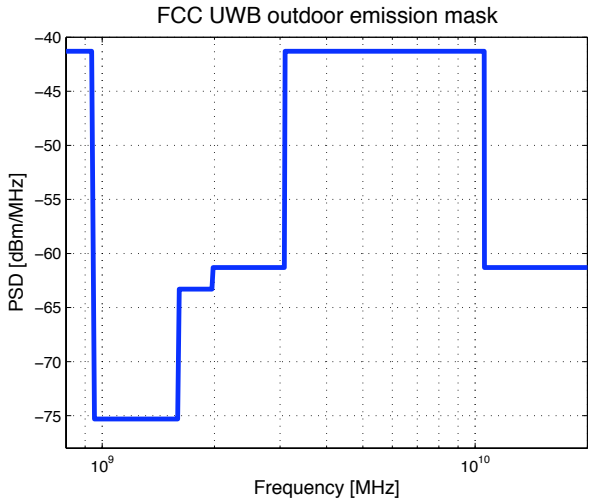

Figure 2.5. FCC outdoor emission mask for UWB devices (FCC,2002).

the gain of the transmitter antenna G_{AT}.

$$EIRP = P_{TX} \cdot G_{AT} \tag{2.8}$$

As seen in Figures 2.4,2.5 EIRP is measured in dBm, that is $10\log_{10}(EIRP_{mWatts})$. The available power of the transmitter P_{TX} is effectively transferred from the transmitter to the antenna when the condition for maximum power transfer between the output impedance of the transmitter Z_{oTX} and the input impedance of the antenna Z_{AT} is verified, $Z_{AT} = Z^*_{oTX}$. An equivalent way of ruling emitted radiations is to impose limits on the field strength V_S in V/m. V_S represents the voltage one should apply to the characteristic impedance of free-space Z_{FS} to obtain an available power P_{TX} after propagation over a distance D. Z_{FS} is 120π that is approximately 377 Ω and in principle it is independent of the frequency. The relation between field strength and available power is

$$EIRP \cong \frac{V_S^2}{377} 4\pi D^2 \tag{2.9}$$

the power defined in (2.8) is an average power, that is, the ratio of the transmitted energy per bit E_b over the bit period T_b. In a binary IR scheme, given the energy of a single pulse E_p, P_{TX} is thus expressed by:

$$P_{TX} = \frac{N_s E_p}{T_b} = \frac{N_s E_p}{N_s T_s} = \frac{E_p}{T_s} \tag{2.10}$$

where $1/T_s$ is the pulse repetition rate. As shown in (2.10), different IR signals can exhibit the same P_{TX} with different pulse energy E_p depending on the repetition rate. At equal average power, signals with low repetition rate may have higher E_p. For equal pulse duration, this is equivalent to saying that the maximum instantaneous power may be markedly different among signals with similar average power. Emission masks impose limits on the PSD of emitted signals, that is on EIRP spectral density, expressed for example in dBm/Hz or dBm/MHz. Emission masks are, however commonly provided in terms of power value at a given frequency, rather than power density values. The values of the mission masks at a given frequency f_c indicates , the maximum allowed EIRP within a measured bandwidth (mb) centered around f_c. For signals having bandwidth B =mb, the maximum allowed EIRP value is exactly the value of $EIRP_{mb}$. For a signal having bandwidth B $\geq mb$, the maximum allowed EIRP is equal to the sum of the $EIRP_{mb}$ values that are provided by the mask corresponding to the frequency range occupied by the signal. In particular we can express a formal definition of $EIRP_{mb}$ for a signal having B=mb as:

$$EIRP_{mb}\frac{B}{mb} = EIRP \simeq \frac{V^2}{377}4\pi D^2 \tag{2.11}$$

Regarding indoor and outdoor UWB systems , the masks limits operation to a -10 dB bandwidth lying between 3.1 and 10.6 GHz, and sets very stringent limits on out-of-band emission masks. The emission masks values of the FCC are reported in tables (2.2.2) and (2.2.2), the rule also specifies a limit on the peak level of emission within a band of 50 MHz bandwidth centered on the frequency f_M, at which the highest radiated emission occurs. The limit is set to 0 $dBm/50MHz$, that is, the

power computed over a frequency range of 50 MHz around f_M is limited to 0 dBm.

Frequency in MHz	$EIRP_{mb}$ in dBm
0-960	-41.3
960-1610	-75.3
1610-1990	-53.3
1990-3100	-51.3
3100-10600	-41.3
Above 10600	-51.3

Table 2.1. Average Power Limits set by FCC in the U.S. for Indoor UWB Devices.

Frequency in MHz	$EIRP_{mb}$ in dBm
0-960	-41.3
960-1610	-75.3
1610-1990	-63.3
1990-3100	-61.3
3100-10600	-41.3
Above 10600	-61.3

Table 2.2. Average Power Limits set by FCC in the U.S. for Outdoor UWB Devices.

In february 2007 the European Community produced a document "**on allowing the use of the radio spectrum for equipment using ultra-wideband technology in a harmonised manner in the Community**". Specifically the EC has chosen to make use of only part of the spectrum that was approved for use in the US in 2002. In Europe UWB communications Part 15 limit of -41.3 dBm/MHz will be applied over the 6.0- to 8.5-GHz frequency range, whereas in the United States the FCC applies this over a broader spectrum from a much lower frequency. It is also applied provisionally until the end of 2010 in the 4.2 to 4.8-GHz range (see table 2.2.2).

Frequency in MHz	max mean EIRP in dBm	max peak EIRP
	density in dBm/MHz	density in $dBm/50MHz$
Below 1600	- 90.0	- 50.0
1600-3400	- 85.0	- 45.0
3400-3800	- 85.0	- 45.0
3800-4200	- 70.0	- 30.0
4200-4800	-41.3 until 12/31/2010	0.0 until 12/31/2010
	-70.0 beyond 12/31/2010	-30.0 beyond 12/31/2010
4800-6000	- 70.0	- 30.0
6000-8500	- 41.3	- 0.0
8500-10600	- 65.0	- 25.0
Above 10600	- 85.0	- 45.0

Table 2.3. Maximum e.i.r.p. densities in the absence of appropriate mitigation techniques, document released by the EC in 2007.

2.3 UWB communications at low data rate

The UWB radio signal is ideally composed of a sequence of pulses that do not overlap in time. With the hypothesis of perfect synchronization between transmitter and receiver, each pulse is confined within a specific time interval, and the pulse itself has finite duration. While Inter-Symbol Interference (ISI) among pulses belonging to the same transmission is ideally absent in the transmitted signal, it might not be so after the signal has travelled through a real channel. Pulses might in fact be delayed by different amounts, and replicas of pulses due to multiple paths might cause ISI. Moreover, if several communications are present in the same time pulses belongings to different communications can collide giving rise to an interference noise called Multi-User Interference (MUI). At the receiver the useful signal is thus corrupted by two additive interference components, the first is the thermal noise introduced by the receiver antenna and receiver circuitry, the second is the MUI introduced by the presence of other transmitting users.

2.3.1 Multi User Interference (MUI)

In this section the MUI problem for multi-access impulse radio UWB (IR-UWB) systems is considered. Since the number of interferers is unknown a priori, a typical assumption that can be made is to consider the multiuser interference as a Gaussian distributed process, this approximation is referred as the Standard Gaussian Approximation (SGA). The SGA relies on the observation that when MUI is provoked by the sum of a large number of users, interference can be treated as an additive Gaussian noise with uniform power spectrum over the frequency band of interest. Under this assumption, receiver tolerance to MUI easily expresses as a function of the average signal to noise ratio at the reference receiver, where noise power is calculated as the sum of thermal noise and average MUI powers. The SGA has two main advantages over the other proposed models (see [36] for a complete survey), it is *simple*, i.e., few system parameters are required for evaluating performance and it is *fast*, i.e., the average BER is provided through an explicit form which can be calculated at a reduced computational cost. The SGA however, is based on the central limit theorem, and provides thus accurate BER estimations only for scenarios with high MUI levels, i.e., for densely populated networks. Provided that the intended scenario comprises only few nodes, the SGA may provide a BER estimations that is optimistic if compared with the theoretical value. In the following the SGA model is briefly described because most of the attention will be focused on a different MUI model, the Pulse Collision Model [36]. Based on the Pulse Collision Model, will be described in section 2.5 the UWB^2 MAC protocol that is used in our simulations.

The Standard Gaussian Approximation

Consider the TH-UWB signal expressed by equation (2.3), from this expression, if we consider that each user is assigned a different TH code, the transmitted signal

is:

$$s_{TX}(t) = \sqrt{E_{TX}} \sum_{j=-\infty}^{\infty} p_0(t - jT_s - c_j T_c - \epsilon a_{\lfloor j/N_s \rfloor}) \tag{2.12}$$

where $p_0(t)$ is the energy-normalized waveform of the transmitted pulses, E_{TX} is the energy of each pulse, T_s is the average pulse repetition period, $0 \leq c_j T_c \leq T_s$ is the time shift of the jth pulse provoked by the TH code, ϵ is the PPM shift, a_x is the xth bit (that is a iid variable) of $\mathbf{a}$, N_s is the number of pulses transmitted for each bit, and $\lfloor x \rfloor$ is the inferior integer part of x. If the channel model is assumed a general flat AWGN model, and perfect synchronization between transmitter TX and receiver RX is assumed, the channel output is corrupted by thermal noise and MUI generated by N_i interfering IR-UWB devices. The received signal thus writes:

$$s_{RX}(t) = r_u(t) + r_{mui}(t) + n(t) \tag{2.13}$$

where $r_u(t)$, $r_{mui}(t)$ and $n(t)$ are the useful signal, MUI, and thermal noise, respectively. As regards $r_u(t)$, one has:

$$r_u(t) = \sqrt{E_u} \sum_{j=-\infty}^{\infty} p_0(t - jT_s - c_j T_c - \epsilon a_{\lfloor j/N_s \rfloor} - \tau) \tag{2.14}$$

where $E_u = \alpha^2 E_{TX}$ and τ is the propagation delay of the channel (that is known at receiver due to the perfect synchronization hypothesis). as regard $r_{mui}(t)$, we assume that all interfering signals are characterized by same T_s but not the same N_s, and thus:

$$r_{mui}(t) = \sum_{n=1}^{N_i} \sqrt{E^{(n)}} \cdot \sum_{j=-\infty}^{\infty} p_0(t - jT_s - c_j^{(n)} T_c - \epsilon a^{(n)}_{\lfloor j/N_s^{(n)} \rfloor} - \tau^{(n)}) \tag{2.15}$$

where $E^{(n)}$ and $\tau^{(n)}$ are received energy per pulse and delay for the nth interfering user. The relative delay $\Delta\tau^{(n)} = \tau - \tau^{(n)}$ is assumed to be a random variable uniformly distributed between 0 and T_s. Both TH codes and data bit sequences are randomly generated and correspond to pseudo-noise sequences, that is, $c_j^{(n)}$ terms

are assumed to be independent random variables uniformly distributed in the range [0,T_s), and $a_x^{(n)}$ values are assumed to be independent random variables with equal probability to be "0" or "1". Finally, signal $n(t)$ in (2.13) is Gaussian noise, with double-sided power spectral density $N_0/2$.

If a coherent correlator followed by a ML detector is the considered receiver. We have that in each bit period (that is $T_b = N_s T_s$ seconds), the correlator converts the received signal of (2.13) into a decision variable Z, which forms the input of the detector. Here Soft is performed, i.e., the signal formed by N_s pulses is considered as a single multi-pulse signal. The received signal is thus cross-correlated with a correlation mask $m(t)$ that is matched with the train of pulses representing one bit. The input of the detector $Z(x)$, for a generic bit a_x, can be thus expressed as follows by the sum of three components:

$$Z(x) = Z_u + Z_{mui} + Z_n \tag{2.16}$$

that are the useful term, the MUI term and the Gaussian noise term, respectively.The bit estimation exploited in the receiver is based on the comparison of the $Z(x)$ value with a predefined zero-valued threshold according to the following rule: if $Z(x)$¿0 decision is "0", decision is "1" otherwise. For independent and equiprobable transmitted bits, the average BER at the output of the detector is:

$$BER = \frac{1}{2} Prob(Z(x) < 0 | a_x = 0) + \frac{1}{2} Prob(Z(x) > 0 | a_x = 1) = Prob(Z(x) < 0 | a_x = 0) \tag{2.17}$$

More specifically, all this terms depend on the transmitted pulse waveform $p_0(t)$. In particular if we consider its autocorrelation function $R_0(t)$:

$$R_0(t) = \int_{-\infty}^{+\infty} p_0(\xi) p_0(\xi - t) d\xi$$

and we define the term $\gamma(\epsilon) = 1 - R_0(\epsilon)$, we have that Z_n, the Gaussian term has zero mean and variance $\sigma_n^2 = N_s N_0 \gamma(\epsilon)$. Under the SGA also the term Z_{mui} is

modeled as Gaussian random variable, and its variance that can be be interpreted as the MUI power at the correlator output at the average operating conditions. Like Z_n, also Z_{mui} depends on the waveform $p_0(t)$, and if we define the term σ_M^2 as:

$$\sigma_M^2 = \int_{-\infty}^{+\infty} \Big(\int_{-\infty}^{+\infty} p_0(t-\tau)(p_0(t) - p_0(t-\epsilon)dt) \Big)^2 d\tau$$

we can write the variance of the MUI term as:

$$\sigma_{mui}^2 = \frac{N_s}{T_s} \sigma_M^2 \sum_{n=1}^{N_i} E^n \tag{2.18}$$

The useful component of the decision variable is Z_u that can be expressed like:

$$Z_u = \begin{cases} +N_s\sqrt{E_u}\gamma(\epsilon), & \text{if } a_x = 0 \\ -N_s\sqrt{E_u}\gamma(\epsilon), & \text{if } a_x = 1 \end{cases}$$

Under the SGA, therefore, the average Bit Error Rate (BER) writes:

$$BER = \frac{1}{2} erfc\left(\sqrt{\frac{1}{2}\left(\Big(\frac{N_s E_u \gamma(\epsilon)}{N_0}\Big)^{-1} + \Big(\frac{N_s T_s \gamma(\epsilon)}{\sigma_M^2 \sum_{n=1}^{Ni}(E^{(n)}/E_u)}\Big)^{-1} \right)^{-1}} \right)$$

The SGA is derived from the central limit theorem and is thus valid only asymptotically.

The Pulse Collision Model

We will firstly briefly introduce the pulse collision model basics as reported in [2], and subsequently describe the model more deeply as can be found in [36]. The time occupied by one single UWB pulse indicated by T_m is defined here as the time interval typically centered on the main lobe in which most of the energy of the pulse at the receiver is concentrated. Typical values for T_m lie between 70 psecs and 20 nsecs depending upon transmitted pulse shape and channel behaviour. Since no synchronization between users is provided, is reasonable to assume that the inter-arrival time of different packets follows a Poisson distribution. Each packet contains

a set of pulses, each subset of N_s pulses carrying the information of one bit. The pulse inter-arrival process is a complex phenomenon that depends on modulation, dithering, codes and so on. To try to express the probability of pulse collision in a closed form, let us assume that the pulse inter-arrival process is a Poisson process itself. Therefore the probability that one or more pulses collide with the useful pulse when P_U packets are transmitted over the air interface by N_U active users can be compared to the Aloha collision probability when the information unit is the pulse instead of the packet. This probability can be expressed as:

$$Prob_{PulseCollision} = 1 - e^{(-2\cdot(P_U-1)\cdot\frac{T_m}{T_s})} \tag{2.19}$$

where T_s is the average pulse repetition period. The number of transmitted packets P_U depends on the number of active users N_U, and if L is the packet length, R_b is the data rate (that is $1/(N_s \cdot T_s)$, where N_s is the number of transmitted pulses per bit) and G is the packet generation rate, its instantaneous value is:

$$P_U = \frac{N_U \cdot L \cdot G}{R_b} \tag{2.20}$$

Assuming that a pulse collision causes a random decision at the receiver the pulse error probability can be expressed as:

$$Prob_{PulseError} = 0.5 \cdot Prob_{PulseCollision} \tag{2.21}$$

Considering that each bit is encoded into NS pulses we assume an error on the bit when more than $N_s/2$ pulse errors occur. This corresponds to assuming a hard receiver detection. Bit error probability is thus expressed by:

$$Prob_{BitError} = \sum_{i=\lceil\frac{N_s}{2}\rceil}^{N_s} \binom{N_s}{i} \cdot Prob_{PulseError}^{i} \cdot (1 - Prob_{PulseError})^{N_s-i}$$

Consider for example a low data rate UWB network in which $N_U = 100$ active users generate packets at a rate G = 10^3 packets/s using a packet length L = 1000 bits.

The data rate R_b $(= 1/(N_s \cdot T_s))$is set to 1 Mbits/s. . In average $P_U = 10$ packets are present in the air interface at a given time. For example if $T_m = 80$ psecs and $N_s = 5$ then $Prob_{BitError}$ $8.47e^{-5}$. Thus the probability of correctly receiving one bit is:

$$Prob_{CorrectBit} = (1 - Prob_{BitError}) \tag{2.22}$$

Here, and in the further simulations we assume that a packet is corrupted if at least one bit error occurs within the packet. Thus, the average probability to transmit a packet successfully is:

$$Prob_{CorrectPacket} = (1 - Prob_{BitError})^L \tag{2.23}$$

Thus, according to the previous example we would have a $Prob_{CorrectPacket}$ of 0.92. $Prob_{CorrectPacket}$ depends upon the number of packets P_U and data rate R_b.

A more detailed detailed description of the pulse collision model, is presented in the recent work [36]. Here the authors present an approximate expression for the average BER at the receiver output for an IR-UWB-TH-PPM system. Let the considered system be the same used for the SGA modeling. The decision variable on which the detector take decision is affected by thermal AWGN and MUI, that is, this variable is composed by three terms:

$$Z(x) = Z_u + Z_{mui} + Z_n \tag{2.24}$$

As described, the SGA considers the Z_{mui} term like and additive random Gaussian term, and the average BER at the output of the detector when all the components are expressed, writes:

$$\begin{aligned} BER &= Prob(N_s\sqrt{E_u}\gamma(\epsilon) + Z_{mui} + Z_n < 0) \\ &= Prob(Z_{mui} < -(N_s\sqrt{E_u}\gamma(\epsilon) + Z_n)) \\ &= Prob(Z_{mui} < -y) \end{aligned} \tag{2.25}$$

where y is a Gaussian random variable with mean $N_s\sqrt{E_u}\gamma(\epsilon)$ and variance $N_s N_0 \gamma(\epsilon)$. In the pulse collision approach, conditional probability of error $Prob(Z_{mui} < -y)$ takes into account collisions between pulses of different transmissions. That is, making the assumption that events of collision are independent of one another we can rewrite:

$$Prob(Z_{mui} < -y) = \sum_{N_c=0}^{N_s N_i} Prob(Z_{mui} < -y|y,N_c) P_{CP}(N_c) \tag{2.26}$$

where N_c is the number of possible collision within a bit interval (the number of possible collision is maximized by the number of all the pulses N_s transmitted by all interferers N_i), and $P_{CP}(N_c)$ indicates where the probability of having N_c pulse collisions within one single bit interval. For independent interferers, $P_{CP}(N_c)$ can be reasonably expressed through the binomial distribution, i.e.,

$$P_{CP}(N_c) = \binom{N_s N_i}{N_c} P_{C_0}^{N_c} (1 - P_{C_0})^{N_s N_i - N_c}$$

where P_{C_0} is the probability that a single interfering device produces a colliding pulse within T_s. P_{C_0} can be computed as the fraction of T_s during which the receiver may be affected by the presence of an interfering pulse and produce non-zero contributions to Z_{mui}, and can thus be expressed as:

$$P_{C_0} = \frac{min(2T_m + \epsilon, 4T_m, T_s)}{T_s} \tag{2.27}$$

where T_m is the length where of the pulse waveform $p_0(t)$, defined as the period of time in which a given percentage of the pulse energy is contained. Compared with the first version of the collision model, this value is more precise than the simplistic T_m/T_s. The BER expression can be evaluated by first computing the conditional BER for a generic y value, and by then averaging over all possible y values, i.e.

$$BER = \sum_{N_c=0}^{N_s N_i} P_{CP}(N_c) \cdot \int_{-\infty}^{+\infty} Prob(Z_{mui} < -y|y,N_c) p_Y(y) dy$$

where p_Y is the Gaussian probability density function (pdf) of y. For the approximation of BER the authors propose a shape for the conditional probability of error, the model that is shown in Figure (2.6) can be expressed by:

$$Prob(Z_{mui} < -y|y,N_c) = \begin{cases} 1, & \text{for } y \leq -Z_{max}(N_c) \\ 1 - \frac{P_{CP}(N_c)}{2}\left(1 + \frac{y}{Z_{max(N_c)}}\right), & \text{for } -Z_{max}(N_c) < y \leq 0 \\ \frac{P_{CP}(N_c)}{2}\left(1 - \frac{y}{Z_{max(N_c)}}\right), & \text{for } 0 < y \leq Z_{max}(N_c) \\ 0, & \text{for } y > Z_{max}(N_c) \end{cases}$$

where $Z_{max}(N_c)$ where is defined as the maximum value for the MUI term Z_{mui}, when N_c collisions have occurred at the reference receiver. The selection of a linear model for the conditional probability of error simplifies the analytical derivation of the BER at the reference receiver and it was selected on the basis of both practical observations and statistical results emerged by simulation.

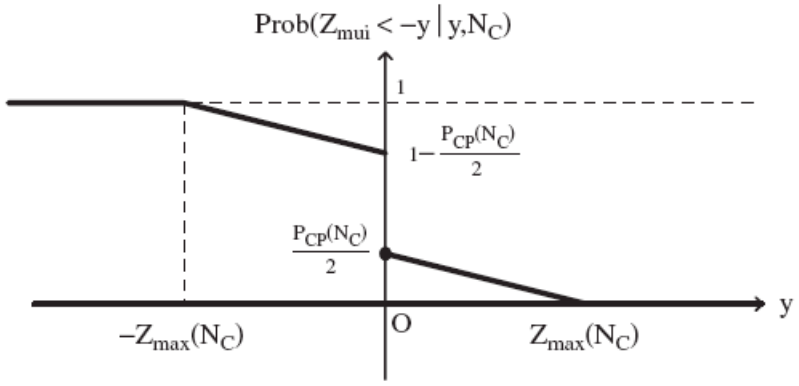

Figure 2.6. Linear model for the conditional probability of error $Prob(Z_{mui} < -y|y,N_c$, given y and N_c according to the Pulse Collision Model.

The authors propose multiple version of the maximum value for Z_{mui}, in our system simulation we adopted an intermediate value for $Z_{max}(N_c)$ that is expressed as follows:

$$Z_{max}(N_c) = \sum_{j=1}^{N_i} \left(\left\lceil \frac{N_c - j + 1}{N_i} \right\rceil \sqrt{E_s^{(j)}} \right) \tag{2.28}$$

where $E_s^{(j)}$ is the received power level of the j interferer. Given maximum value for Z_{mui}, we can finally find the following approximate expression for the average BER at receiver output:

$$BER \approx Q\left(\sqrt{\frac{N_s E_u}{N_0} \gamma(\epsilon)} \right) + \sum_{N_c=0}^{N_i N_s} \frac{P_{CP}(N_c)^2}{2} \Omega\left(\frac{N_s E_u}{N_0} \gamma(\epsilon), \frac{Z_{max}(N_c)^2}{N_s N_0 \gamma(\epsilon)} \right) \tag{2.29}$$

where the Ω function is:

$$\Omega(A,B) = Q(\sqrt{A} - \sqrt{B}) + Q(\sqrt{A} + \sqrt{B}) - 2Q(\sqrt{A}) \tag{2.30}$$

The BER expression includes a first term that only depends on signal to thermal noise ratio at RX input, and a second term accounting for MUI. Note that for computing (2.29), no additional information with respect to the BER computation with the SGA is requested. The result in (2.29) provides an explicit analytical expression for the average BER at the reference receiver in the case of propagation over an AWGN channel. As the authors state this model remains valid in the presence of multipath-affected channels, because a multipath channel can be modeled an increased number of pulses that collide in air, thus, by expanding expressions of the probability of having N_c colliding pulses and the maximum allowable value of $Z_{max}(N_c)$, multipath channels can be managed. The proposed model is validated by system simulations, different scenarios are considered for different values of N_s and varying the number of interferers N_i. By simulation is shown that increasing the number of pulses per bit N_s, does not provide better performance, because if

one wants to receive a certain value of energy per bit called E_b while increasing N_s, (not varying other parameters such average pulse repetition period T_s), the useful energy E_u is reduced, since we can write:

$$E_u = \frac{P_{TX} \cdot T_s}{channel\_pathloss} \tag{2.31}$$

while it is true that:

$$E_b = E_u \cdot N_s \tag{2.32}$$

As reported in the relative section, we can confirm by simulation that if we increase N_s but we maintain constant the product $(N_s \cdot T_s)$, that is, we maintain constant the bit rate $R_b = 1/(N_s \cdot T_s)$, the system performance in terms of BER are still degrading. So receiver performance do not depend only on the amount of useful energy per bit which is collected at the receiver, but it also depends on how many pulses are used for transmitting such energy. By simulation is shown that the BER estimation based on Pulse Collision fit simulation data while SGA underestimates BER. In general the Pulse Collision Model provides an higher accuracy in estimating BER than the SGA either for power-controlled either for power-unbalanced systems.

2.4 Narrowband interference (NBI) onto UWB systems

Provided that UWB spectrum width spans from 3.1GHz up to 10.6 GHz, it is unavoidably overlapped with the spectra of existing narrowband technologies that transmit within this range; thus, it necessary to quantify the amount of potential mutual interference between different coexisting technologies. Therefore, significant research has been carried out aimed at evaluating this the effect of UWB signals on narrowband systems. As far as power levels are concerned, on the one hand UWB

has significant constraints imposed by the regulatory agencies while having an extremely wide bandwidth, on the other narrowband signals occupy a much smaller bandwidth, where their power spectrum is very high, thus the influence of narrowband signals on the UWB system can be significant, and in the extreme case, these signals may jam the UWB receiver completely.

To guarantee the coexistence between UWB signals and already-existing narrowband systems, effective interference caused by UWB on these technologies can't be neglected. Several studies on this subject are available in the literature, for example in [37] an extended simulation study on the interference on UMTS, GPS, DCS1800, and Fixed Wireless Systems is provided.

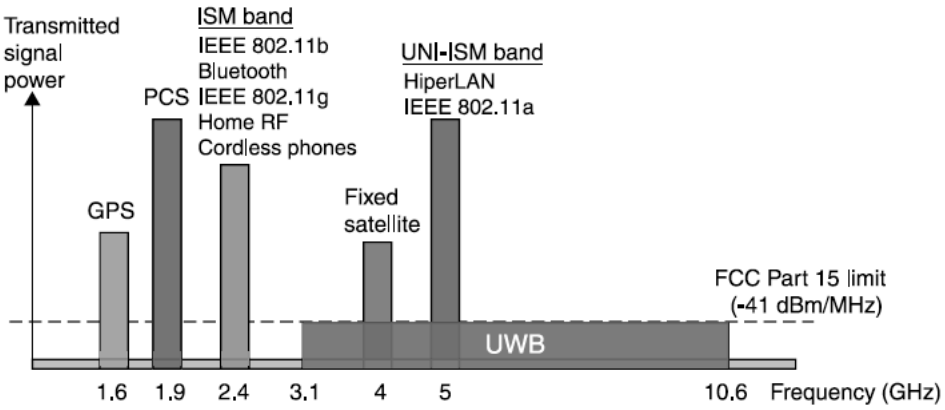

Figure 2.7. Spectrum overlapping of the narrowband interferers in UWB systems.

Despite the fact that spectrum interference is reciprocal, in this work we are more interested in the effects that other already-existing systems have on UWB signals.

Even though narrowband signals interfere with only a small fraction of the UWB spectrum, due to their relatively high power with respect to the UWB signal, the performance and capacity of UWB systems can be considerably affected. Recent

studies show that the BER performance of the UWB receivers is greatly degraded due to the impact of narrowband interference (NBI).

NBI is a problem also for other wideband systems like Code Division Multiple Access (CDMA) systems, but while in this systems NBI is partially handled with the processing gain and employing several interference cancellation techniques such as notch filtering or minimum mean square error (MMSE) detectors, NBI suppression in UWB is a more challenging problem because of the restricted power transmission and the higher number of narrowband interferers due to the extremely wide band occupied. Moreover, in carrier modulated wideband systems, before demodulating the received signal both the desired wideband and the narrowband interfering signals are down-converted to the baseband, and the baseband signal is sampled above the Nyquist rate. Sampling at the Nyquist rate allows numerous efficient narrowband interference cancellation algorithms based on advanced digital signal processing techniques to be employed. However, in UWB, the desired signal is already in the baseband, while the narrowband interferer is in radio frequency (RF), furthermore the signal can not be sampled at the Nyquist rate with the existing technologies. Therefore existing NBI cancellation techniques for wideband systems can not be applicable for UWB. Given the low complexity requirements in both hardware and computation, and considering the other limitations such as low-power and low-cost transceiver design in many UWB applications, the NBI problem needs to be handled more carefully, and effective techniques that are able to cope with NBI need to be developed. Most of the proposed methods effective for UWB, can be classified as NBI avoidance and NBI cancellation techniques, all these techniques require the statistical identification of the NBI. NBI avoidance methods are based on avoiding the transmission over the frequencies of strong narrowband interferers or by modeling the signal spectrum by pulse shaping. The cancellation techniques,

on the other hand, aim at eliminating the effect of NBI on the received UWB signal.

Regarding the jamming resistance, impulse radio UWB behaves very similar to Direct Sequence Spread Spectrum (DSSS), where this resistance is provided by the processing gain, which is obtained by spreading. The larger the spreading ratio (the ratio of bandwidths of the spread signal and the original information), the higher the processing gain, and hence, the better jamming resistance is obtained. At the receiver, the transmitted spread spectrum signal and the narrowband interferer go through a despreading operation, where the receiver takes the wideband spread spectrum signal and collapses it back to the original data bandwidth, while spreading the interferer to a wide spectrum. As a result, within the data bandwidth, the effect of interferer is mitigated, a fact which is referred as the jamming resistance or the natural interference immunity of the spread spectrum signals. Similar to the DSSS systems, impulse radio based UWB also has inherent immunity to NBI. Time-hopping UWB systems can be considered as an example. The processing gain of TH-UWB signal is mainly obtained by transmitting very narrow pulses with a very low duty cycle. During the reception of TH-UWB signals, using a matched filter that basically operates as a time gate (i.e., lets the UWB signal along with interference pass over the duration of the expected pulses, and blocks the rest of the received signal), the power of the interfering signal is reduced significantly. As a result, jamming resistance against NBI is obtained. Note that there will be still partial interference at the output of the matched filter depending on the processing gain, the power of the interferer, and other factors.

As reported in [38] and in [39] the narrowband interference that effects UWB systems can be modeled in various ways. One of the commonly used models considers NBI as a single tone, leading to

$$i(t) = A\sqrt{2P_i}cos(2\pi f_c t + \phi_i) \tag{2.33}$$

where A denotes the channel gain, P_i is the average power, f_c is the frequency of the sinusoid, and ϕ_i is its phase. Another example for Narrow Band Interference model is to consider it as an additive Gaussian noise. The corresponding model is a zero-mean Gaussian random process and its power spectral density is as follows:

$$S_i(f) = \begin{cases} P_{int}, & f_c - \frac{B}{2} \leq |f| \leq f_c + \frac{B}{2} \\ 0, & \text{otherwise} \end{cases}$$

where B and f_c are the bandwidth and the center frequency of the interferer, respectively, and P_{int} is the power spectral density. The received signal can be shown as

$$r(t) = v(t) + i(t) + n(t) \tag{2.34}$$

where $v(t)$ denotes the UWB signal, $i(t)$ is NBI, and $n(t)$ is the additive white Gaussian noise (AWGN) with a PSD of N_0. To identify the NBI within the received signal is extremely useful to analyze the correlation between the samples of the signal. Since the narrowband signal has a bandwidth much smaller than the coherence and width of the channel, the time domain samples of the NBI are highly correlated with each other. Therefore, for the investigation of the narrowband interferers, the correlation functions are of primary interest, rather than the time- or frequency-domain representations. If NBI is modeled as single tone, the correlation between the samples of the received signals can be shown as

$$R_i(\tau) = P_i|A|^2 cos(2\pi f_c \tau) + N_0\delta(\tau) \tag{2.35}$$

where τ is the duration between the received samples. In the case of band limited interferer, the correlation function becomes

$$R_i(\tau) = 2P_{int}Bcos(2\pi f_c\tau)sinc(B\tau) + N_0\delta(\tau) \tag{2.36}$$

For system simulations present in the relative chapter of this work NBI on UWB system is considered, in particular we assumed that the narrow band interferer was modeled as an additive Gaussian Noise.

2.5 MAC Protocols for Low Data Rate UWB

In this section Multiple Access protocols for low data rate Ultrawide Band systems are reported. More specifically, we will investigate those protocols for MAC layer that are specifically designed for Low data-rate scenarios. Basics principles of the *IEEE 802.15.4* networks MAC protocol will be described; subsequently we introduce the *UWB*^{2}:Uncoordinated, Wireless, Baseborn Medium Access for UWB Communication Networks protocol [2] which is specifically designed for the special case of low data rate IR-UWB networks. IR-UWB signals have an high temporal resolution, thus an high degree of robustness to MUI is provided, in particular for low data rate applications [34]. As a consequence, an uncoordinated Medium Access Control like an Aloha-like MAC protocol can be adopted. Thanks to the resilience to MUI offered by impulse radio, correct reception for multiple simultaneous links can be obtained. An Aloha-like approach may also favour lowering costs, since it does not rely on specific physical layer (PHY) functions, such as carrier sensing, and may thus be adapted with little effort to different PHYs. Since UWB^2 protocol was the MAC protocol we chose for the simulated system presented in this work we will describe this protocol more deeply.

IEEE 802.15.4 MAC protocol

The IEEE 802.15.4 [40] is a MAC protocol intended for low data-rate networks with distances between nodes hardly greater than 30 meters. This protocol can be operated in a beacon enabled mode or a non-beacon-enabled mode that is with or without a Time Division basis. Network nodes are organized in Personal Area Networks (PANs) with a Coordinator node. The medium access within a PAN is controlled by the PAN coordinator. Two different topologies are possible within a PAN, *star topology* and *peer-to-peer topology*. In the non TDMA mode, users in a PAN communicate with each other based on the unslotted CSMA/CA. In the beacon enabled mode, the PAN Coordinator define a Superframe that has an active period and an optional inactive period. The Superframe structure is divided into 16 slots, this length is specified as Beacon Interval (BI); the Superframe structure is depicted in Figure(2.8). Superframe composition is no briefly provided:

- The first slot is always occupied by the beacon, that is used by the Coordinator to broadcast information to all devices in the PAN
- Subsequent slots compose the Contention Access Period (CAP) that is divided, that is used by terminals to send data to other devices or to the Coordinator in a slotted CSMA/CA fashion
- In order to support low-latency applications, the PAN coordinator can reserve one or more slots that are assigned to devices running such applications without need for contention with other devices. Such slots are referred to as guaranteed time slots (GTS), and they form the contention-free period (CFP) of the Superframe

During the inactive period, the coordinator and nodes shall not interact with its PAN and may enter a low-power mode.

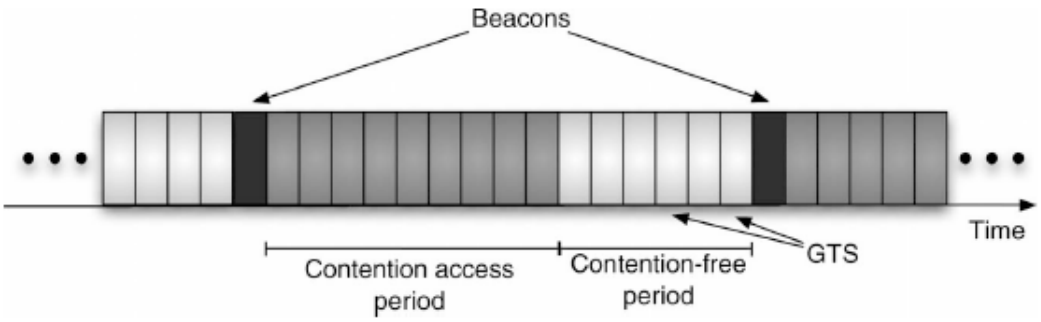

Figure 2.8. An example of Superframe structure for 802.15.4 MAC.

If TDMA is not adopted, beacons are no longer needed for the definition of a slotted time axis, but they are still required for broadcasting the ID of the PAN and allow association of new devices. Unslotted CSMA/CA makes peer-to-peer data exchange difficult, since no common synchronization is available between devices, and in the Standard it is not provided any specific synchronization procedure.

UWB^2 MAC protocol

The Uncoordinated, Wireless, Baseborn Medium Access for UWB Communication Networks referred as UWB^2 [2], is a MAC protocol specifically designed for Impulse Radio Ultra Wideband systems. The multiple access scheme is based on the combination of a common control channel provided by a common Time-Hopping (TH) code with dedicated data channels associated to transmitter specific TH codes. The proposed protocol also takes into account synchronization requirements, in fact each transmitted packet has a synchronization trailer part, composed by a certain number M of pulses (M is known a priori by receivers and depends on the environment conditions). To obtain synchronization with the transmitter the receiver use a dedicated correlator that is continuously searching for the synchronization trailer. This

correlator generates a peak in the presence of a synchronization trailer at its input. When conditions are favourable, i.e. required SNR is met, the peak exceeds a given threshold, and triggers the detection circuit.

(UWB)2 is a multi-channel MAC protocol. In multi-channel protocols the overall available resource is partitioned into a finite number of elements. Each element of the resource partition corresponds to a channel. According to the definition of resource, a channel can therefore corresponds to:

- A time slot, as in TDMA
- A frequency band, as in FDMA
- A code, as in CDMA

In multi-channel CDMA MAC algorithms, commonly referred to as multi-code, each channel is associated a different code, thus the two major weaknesses are the MUI caused by the contemporary transmission of different packets from different users using different codes, and the collisions on the code, caused by the selection of the same code by two different transmitters within radio coverage. Robustness to MUI can be increased adopting low correlated codes while for different channels codes assignments 4 main solutions are possible:

1. *Common Code*: all terminals share the same code, relying on phase shifts between different links for avoiding code collisions. If phase shifts are too small this solution collapses into the single Aloha channel.

2. *Receiver Code*: each terminal has a unique code for receiving, and the transmitter tunes on the code of the intended receiver for transmitting a packet. Receiver complexity is thus reduced.

3. *Transmitter code*: each terminal has an unique code for transmitting, and the receiver tunes on the code of the transmitter for receiving a packet. Receivers must be able to listen to all possible codes in the network.

4. *Hybrid*: a combination of the above schemes.

Among these solutions, UWB^2 adopts an Hybrid scheme for the specific case of a TH-IR UWB system based on the combination of a common control channel, provided by a Common TH code, with dedicated data channels associated to Transmitter TH codes. The adoption of the Hybrid scheme is motivated by the authors as it simplifies the receiver structure (data transmissions and corresponding codes are transmitted on the common channel) and it provides a common channel for broadcasting that is a key property for the operation of higher layers protocols. Broadcast messages are for example required for routing and distributed positioning protocols. The packet exchange procedure described below show that UWB^2 also exploits the ranging capability offered by UWB. Distance information between transmitter and receiver is in fact collected during control packets exchange. Such information can enable optimizations of several MAC features, and allow the introduction of new functions, such as distributed positioning.

In the following procedure is assumed that, at each terminal T, MAC Protocol Data Units (MACPDUs) resulting from the segmentation/concatenation of MAC Service Data Units (MACSDUs) are stored in a transmit queue. It is also assumed that T is able to determine how many MACPDUs in the queue are directed to a given receiver R.

The transmission procedure Terminal T periodically checks the status of the its MACPDUs queue and if there are data to transmit the terminal enable the transmission procedure which can be described as follows:

1. The ID of the intended receiver R is extracted from the first PDU in the queue;

2. T determines the number N_{pkts} of MACPDUs in the queue directed to R;

3. T checks if other MACPDUs were sent to R in the last T_{active}seconds. If this is the case, T considers R as an Active receiver, and moves to step 5 of the procedure;

4. If R is not an Active receiver, T generates a Link Establish (LE) packet. The LE packet is composed by the following fields (see Figure 2.9 a)):

   - SyncTrailer, used for synchronization purpose
   - Tx NodeID, the MAC ID of transmitter T
   - RxNodeID, the MAC ID of receiver R
   - TH Flag, this flag is set to **true** if the standard TH code associated to TxNodeID will be adopted for transmission of data PDUs. The flag is set to false if a different TH code is going to be adopted
   - TH Code (optional), if the TH Flag is set to **false**, the information on the TH-code to be adopted is provided in this field.

5. Terminal T sends the LE packet and waits for a Link Confirm (LC) (see Figure 2.9 c)) response packet from R;

6. If the LC packet is not received within a time T_{lc}, the LE packet is re-transmitted for a maximum of N_{lc} times, before the transmission of the MACPDU is assumed to be failed;

7. After receiving the LC packet, T switches to the TH code declared in the LE packet and transmits the data packet. The data packet is composed of (see Figure 2.9 b)):

   - SyncTrailer, used for synchronization purposes

- Header, including the fields TxNodeID, RxNodeID, PDU_{num} and N_{pkts}
- Payload, containing data information

8. Once the transmission is completed, T checks again the status of the data queue, and repeats the procedure until all MACPDUs in the transmit queue are served.

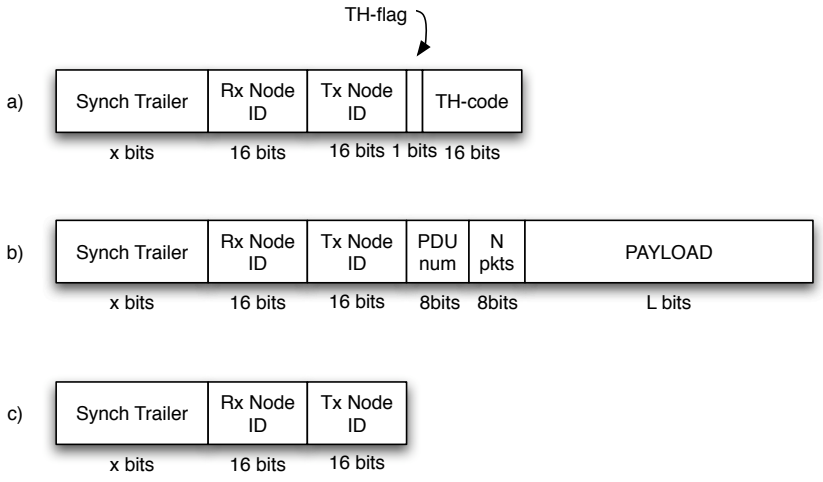

Figure 2.9. UWB^2 MAC protocol packet structures, a) Link Establish (LE) packet, b) Data packet and, c) Link Confirm (LC) packet.

Reception procedure This is the procedure a terminal R in Idle state executes when while listening to the Common TH code, a SyncTrailer is detected.

1. R checks the Rx Node ID field. If the value in the field is neither the MAC ID of R nor the broadcast ID, the reception is aborted and the reception procedure ends;

2. Since in the following we are not considering broadcast packets, let us assume that the Rx Node ID contains the MAC ID of R. In this case, since R is

assumed in Idle state, MACPDUs directed to this terminal will necessarily be LE packets;

3. Following the reception of a LE packet, R creates a LC packet, composed of (see Figure 2.9 c)):
   - SyncTrailer, used for synchronization purposes
   - TxNodeID, the MAC ID of T
   - RxNodeID, the MAC ID of R
4. R sends the LC packet and moves in the Active state, listening on the TH code indicated in the LE packet. If no data packet is received within a time T_{data} the receiver falls back to Idle state and the procedure ends;
5. When a data packet is received, R processes the payload, and extracts N_{pkts} from the header. If $N_{pkts} > 0$, R remains in Active state, since at least N_{pkts} more data packets are expected to be received from T. If $N_{pkts} = 0$, R goes back to the Idle state.

It should be noted that the above procedures are related to the setup of a single link. During the reception procedure for example R also keeps on listening to the common code. A terminal in fact can act as a receiver on one or more links while acting as a transmitter on other links.

Chapter 3

convergence IR-UWB

3.1 convergence IR-UWB

Given the strong similarities between impulse radio UWB and wireless optical, the combination of the two technologies can provide strong benefits and overcome limitations characterizing both systems. In this section we will propose the combination of the two physical layers by adopting a common medium access control protocol. The choice of the most suitable physical layer can follow several strategies, specifically we consider two different casses: minimization of the overall bit error rate and minimization of the power consumption of the nodes (i.e. the higher the interference level, the higher the number of necessary retransmissions to obtain the same BER target).

While optical communication systems can operate everywhere without any specific regulatory permission, UWB radio, is subject to strong power limitations due to its wide band that can potentially overlap with pre-existing wireless services. As a consequence UWB links are sensible to the effect of strong narrowband interferers that can jam the UWB signal and adversely affect performance (see section 2.4).

This issue is particularly relevant in specific application scenarios where such narrowband interferers are inherently present: this is the case for example of medical premises, where diagnostic machines can emit RF radiations while operating, and of industrial environments. In such scenarios network performance can be significantly improved thanks to the adoption of an alternative physical layer solution based on Diffuse Wireless Optical (DWO) technology.

Furthermore, the similarities between UWB and DWO signal formats and characteristics suggest that medium access control protocol schemes proposed for IR-UWB can be used for both technologies, thus leading to a straightforward convergence of UWB and DWO. In this work we evaluate the feasibility of this approach, by proposing a solution for combining the two technologies by means of an environment-aware physical layer selection strategy. The performance of the two physical layers solutions is evaluated by simulations in order to determine the potential performance increase guaranteed by the adoption of the proposed strategy.

3.2 Switching physical layer

The physical layer of the proposed dual system is able, if necessary, to switch from a technology to another according to a predefined rule. The optical part of the considered system is a Diffuse Wireless Optical physical layer with an OOK modulation. Since we are interested in low cost transmission systems, the considered transmitter is an infrared LED with wavelength of possibility of 850 nm (instead of, for example, a more expensive laser diode). We evaluate the performance of the DWO system both in the case of absence of a channel coding and in the case of Optical Orthogonal Codes. Provided simulations will show the improvements due to the presence of the code. On the other hand, the UWB physical layer part, is a 2 level PPM system, that uses Time Hopping codes.

As previously mentioned, we propose two different physical layer switching strategies. The first is aimed at straightforwardly minimizing the whole system BER, therefore, the selection is based on the rule:

$$PHY = argmin\{BER_{UWB}, BER_{DWO}\} \tag{3.1}$$

where BER_{UWB} is the bit error rate measured on the UWB physical layer and BER_{DWO} is the bit error rate measured on the diffuse optical wireless physical layer. Both BER values can be measured either on the basis of previous data packets exchange, or by means of beacon packets sent on the two physical layer interfaces. The exact definition of the procedure for obtaining such measurements is outside the scope of this work, and is left for future investigation.

The goal of the second switching strategy is minimizing the consumed energy of each node due to the transmissions and receptions of packets. In this case the selection of the physical layer is carried out according to the following rule:

$$PHY = argmin\{C_{UWB} \cdot BER_{UWB}, C_{DWO} \cdot BER_{DWO}\} \tag{3.2}$$

where C_{UWB} and C_{DWO} are the cost of the transmission of one bit, for the UWB PHY and the DWO PHY, respectively. This case can be considered as a general case provided that the former strategy can be obtained setting $C_{UWB} = C_{DWO} = 1$. The basic principle of this latter strategy, is that if transmitting a bit using the UWB physical layer has a higher energy cost than transmitting the same bit with DWO physical layer, DWO should be preferred to some extent also when $BER_{DWO} > BER_{UWB}$. The value of the two coefficients would thus depend on hardware, physical layer settings (e.g. code selection) and MAC settings (retransmission strategy and MAC layer FEC coding). In the following part of this work system simulation results are provided for the first switching strategy, that is we consider both the cost coefficient

to be equal to one. The resulting system is thus aimed at minimizing overall BER i.e. the chosen physical layer is the one that provides a lower bit error rate.

3.2.1 Energy consumption for UWB systems

Aimed at evaluating the energy consumption due to the transmission and/or reception of one packet, we study the case of an UWB system. Our goal is to evaluate how much energy is consumed by a single node of the network when it is involved in transmitting or receiving one packet. We based our model on the framework for energy-evaluation defined in [41]; here the authors show how power consumption depends on hardware characteristics of the transceiver, physical layer settings (e.g. code selection) and MAC settings like retransmission strategy and MAC layer coding. We now describe the energy consumption rule for the transmission of a packet followed by the consumption for a reception. For our UWB system, the energy consumed by a node when a packet of size $Packet_{size}$ is sent at low bitrate, can be expressed by the sum of two main components, the startup energy $E_{startup}$ and the effective transmission energy:

$$Energy_{TX} = E_{startup} + Packet_{size} \cdot \left(E_{TX_{perbit}} + E_{TXprop} \cdot d^{\alpha} \right) \tag{3.3}$$

where $E_{TX_{perbit}}$ is the energy that is necessary to transmit a single bit, E_{TXprop} is the dissipated energy of the transmitting amplifier, d is the distance between transmitter and receiver and α is the exponent of the power attenuation low of the environment. The energy necessary for the reception of a packet of size $Packet_{size}$ for the same system is expressed by:

$$Energy_{RX} = E_{startup} + Packet_{size} \cdot E_{RX_{perbit}} \tag{3.4}$$

In the original model (see [41]) also a term that depends on the decoding algorithm is used, however since we do not consider channel coding, we decided to neglect that

term. We adopted the presented consumption model with a low data rate UWB system in the presence of narrow band interferers, as it is shown in Figure (4.5), as the interfering power increases the energy consumption grows up because of the higher number of retransmissions (and receptions) necessaries.

3.2.2 Optical Quantum Limit

The considered optical receiver is a direct detection system, so the detector converts the received power into an electrical current. The received signal at the optical detector output is always non-negative (because power is always non-negative) and random due to the random arrival times of photons. This is not a flaw in the detector, but rather is a fundamental law of physics as dictated by quantum mechanics. Quantum effects are present but insignificant at microwave frequencies and below, but are important at optical frequencies typically in the near-infrared band. If we consider an ideal receiver in which all impairments are absent, and we want to determine the error probability, there is a fundamental limit we cannot neglect, the *Quantum Limit* [42].

Consider a single transmitter-receiver couple. If we were magically able to eliminate all other sources of noise, and were able to reliably detect a photo-electron in the receiver circuitry, then we could use the following receive criterion: no pulse was transmitted if we receive zero photo-electrons, and a pulse was transmitted if we receive one or more photo-electrons in the symbol interval. If we assume that no dark current is present and a perfect quantum efficiency ($\eta = 1$, that is all the light energy is converted in electrical energy), the arrival rate of photo-electrons is:

$$\lambda(t) = \frac{P(t)}{h \cdot \nu} \tag{3.5}$$

where $P(t)$ is the received optical power and $h \cdot \nu$ is the energy of one photon (h is

the Planck's constant and ν is the frequency of one photon). The number of photo-electrons observed during a symbol interval is a Poisson distributed random variable with parameter Λ, where Λ is the integral of $\lambda(t)$ over the symbol period. Thus, when a pulse is transmitted ($\Lambda > 0$) the probability of n received photo-electrons is:

$$p(n) = \frac{\Lambda^n e^{-\Lambda}}{n!} \tag{3.6}$$

Since the integral of power is energy,

$$\Lambda = \frac{E_b}{h \cdot \nu} \tag{3.7}$$

where E_b is the total received energy in the symbol interval. Since $h \cdot \nu$ is the energy of one photon, another interpretation of Λ is the average number of photons arriving at the detector in one symbol interval.

Quantum effects are negligible at microwave frequencies because since this frequencies are about five orders of magnitude smaller than optical frequencies, the energy per photon is five orders of magnitude smaller, and for a given received pulse energy the average number of photons is five order of magnitude larger. Since that the variance of the Poisson distribution in (3.6) is equal to the mean, the standard deviation is the square-root of the mean. The width of the distribution, as defined by the standard deviation divided by the mean, approaches zero as the mean gets large. Thus, for a very large number of received photons, the width of the Poisson distribution approaches to zero, and the randomness due to quantum effects becomes negligible.

According to [42] for idealized receiver with no interferences no error can be made if no pulse is transmitted, since precisely no photons will be received. Hence the only error that is possible result if a pulse is transmitted and no photons are

observed. The probability of errors in this case is:

$$P_e = 0.5 \cdot p(0/1) = 0.5 \cdot e^{-\Lambda} \tag{3.8}$$

where the factor 0.5 reflects the fact that no errors occur if no pulse is transmitted (under hypothesis that bits are equally likely).

3.2.3 Modified-Quantum Limit

Aimed at building a more realistic model, we studied realistic pathloss distributions for wireless optical channels [43], [23]. Specifically, to evaluate LOS and NLOS path channel gain we exploit results in [23]. In the case of no multipath dispersion we can reasonably consider that the *Quantum limit* can be extended as follows: the probability of detecting 0 if a 1 was transmitted depends on the interfering received energy:

$$p(0/1) = e^{-\left(\frac{E_u/A_u + 0.5 \cdot \frac{T_m}{T_s} \cdot \sum_{i=1}^{N} E_{interf(i)}/A_i}{h\nu}\right)} \tag{3.9}$$

where N is the total number of interfering signals, E_u is the received energy of the reference signal, A_i is the attenuation of the channel between the N+1 transmitters and the reference receiver, h is the Plank's constant and ν is the frequency at which the optical system is working (we chose the value corresponding to a LED that works at 850 nm, that is 3.529x$10^{14} Hz$). T_m is the time duration of the transmitted pulse and T_s is the average pulse repetition period, i.e. each pulse is transmitted within a time window of duration T_s.

The probability of detecting 1 even if a 0 was transmitted is no more zero (as claimed by *Quantum limit*), in fact due to the presence of interferers we have a new additive term representing the fact that even if no pulses where sent by reference transmitter, the receiver can detect the contribution of interferers, we thus have:

$$p(1/0) = \left(1 - e^{-\left(\frac{0.5 \cdot \frac{T_m}{T_s} \cdot \sum_{i=1}^{N} E_{interf(i)}/A_i}{h\nu}\right)}\right) \tag{3.10}$$

So the overall bit error probability can be expressed by sum of two equally like contributions:

$$P_e = 0.5 \cdot p(0/1) + 0.5 \cdot p(1/0) \tag{3.11}$$

According to the proposed performance evaluation method based on the quantum limit approach, varying the time duration of the optical transmitted pulse T_m, that is choosing different types of LEDs, will influence the bit error rate. In Figure (3.1) a simulation result of this effect is shown. In the Figure we consider two different scenarios, the first with all nodes of the network in visibility ($NLOS_{prob} = 0$) and the second in which some of the nodes can not communicate with the direct link, that is for all the nodes there is a given probability ($NLOS_{prob} = 0.3$) that they are not in visibility. The simulated networks are composed by 10 nodes randomly positioned within a square room of 12mx12m, the average transmitter power is fixed at 1mW and the transmission rate of each node is 10kbps. As can be seen, if T_s is constant, increasing the pulse duration increases the BER in both cases.

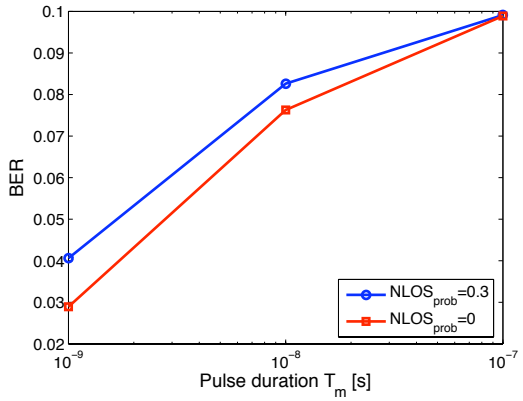

Figure 3.1. BER variation due to a different time duration of the transmitted optical pulse with the same average transmitted power of 1mW and 10 nodes randomly positioned within a square room of 12mx12m.

3.2.4 Diffuse wireless optical channel performance using OOC

For the performance evaluation of a DWO system that adopts optical orthogonal codes we refer to [9] were Inter Symbol Interference (ISI) and MUI are considered. The adopted indoor channel impulse response follows the *ceiling bounce model* described in section (1.2.2) that is expressed by equation (1.13). According to [15] with an OOC code (n,w,1,1) the maximum number of user that can transmit at the same time is limited by:

$$N \leq \left\lfloor \frac{n-1}{w(w-1)} \right\rfloor \tag{3.12}$$

where n is the number of chips of the code and w is the weight of the code, that is the number of "1" within the n chips. If a synchronous system is considered and the hypothesis that the received interfering power is equal to the desired power, we define the amount of interference due to ISI that the chip kth causes on the chip jth as $p_i(k,j)$. Because of ISI also the desired signal introduces some interference, that is the interference produced by the desired chip kth on the desired chip jth, this is expressed by: $p_d(k,j)$. Expressions for $p_i(k,j)$ and $p_d(k,j)$ are given by:

$$p_i(k,j) = p_d(k,j) = h_{j-k} \qquad (k \leq j) \tag{3.13}$$

where h_k is the equivalent discrete-time impulse response of the system sampled at rate $1/T_c$ where T_c is the chip duration. An expression of h_k is:

$$h_k = pT_c \otimes h(t) \otimes g(t) \tag{3.14}$$

where pT_c is a rectangular pulse with duration $0 \leq t \leq T_c$ an $g(t)$ is the transmitted pulse waveform. The number of user that are causing interference is referred as p_{MUI}. If the interfering signal stands exactly on the same chip of the desired signal $p_{MUI} = h_0$ otherwise $p_{MUI} = 0$. The effect of multipath distortion is spreading the signal over different chips causing thus ISI on the received signal. The amount of interference that a single user can perceive on his desired signal can be evaluated

considering the all the possible combination of the codes. When the desired user transmits 0 or 1, we denote the amounts of interference to the desired signal by P_0 and P_1 respectively. Expressions of P_0 and P_1 are:

$$P_0 = \sum_{j=0}^{n-1} \sum_{k=0,k\neq j}^{n-1} p_i(k,j) + p_{MUI} \tag{3.15}$$

$$P_1 = \sum_{j=0}^{n-1} \sum_{k=0,k\neq j}^{n-1} \{p_i(k,j) + p_d(k,j)\} + p_{MUI} \tag{3.16}$$

At the receiver the signal is correlated and only the interferences on the same chips of the desired signal are added. These added interferences can be denoted by P_{m0} and P_{m1} respectively. The mean BER can be evaluated averaging all the possible combination of w "1" within n chips called Δ and be expressed by:

$$BER = \frac{1}{F^{(N-1)}2^{3(N-1)}} \sum_{i=1}^{\Delta} \left\{0.5 \cdot Q\{\gamma(2b - \frac{P_{m0,i}}{w}) + 0.5 \cdot Q\{\gamma(2A - \frac{2P_{m1,i}}{w} - 2b)\}\right\} \tag{3.17}$$

where

$$\gamma = \frac{G_0 P_{TX} \rho}{2} \sqrt{\frac{nT_c}{w\sigma^2}} \tag{3.18}$$

where b is the receiver threshold of the receiver, N is the possible number of users depending on the code, A is the received signal in the desired chip place, σ^2 is the power spectral density of the thermal noise present at the output of the photodetector, P_{TX} is the average transmitted power, and ρ is the responsivity of the receiver.

3.3 MAC for Low Data Rate Impulsive systems

Wireless access is not only the action of accessing, that is connecting to, a fixed network but also but more in general, the action of accessing the wireless medium. This is in fact, the available resource that has to be shared among the nodes of the

network is the wireless medium.

The wireless access can be centralized or distributed, in the case of centralized the resource available to the system is managed and controlled by a central unit that is the network coordinator. All the units that want to join, leave or transmit in the network must refer to this unit. In decentralized access systems, all nodes are hierarchically equivalent (there is not a central unit with MAC access functions) and they can cooperate for the purpose of resource sharing. A typical example of centralized access network is the IEEE 802.11 system in which the role of the central unit is covered by an Access Point unit (or Hot Spot) which is an element connected to the fixed network and that coordinates the access of wireless devices by managing the resource available in the system for transmissions. Other examples are cellular networks like GSM or UMTS networks. A typical example of decentralized access networks is an ad-hoc network. In ad-hoc networks nodes can be cooperative or non-cooperative in finding routes to reach other nodes, in controlling the transmitting power aimed at not interfering among them or in organizing the structure of the network.

The MAC protocol we used in our simulations is the UWB^2 protocol that has been already described in the section (2.5). This protocol is specifically designed for IR UWB signal, however, thanks to the impulsive nature of optical signals it can reasonably be exploited in the studied context.

Chapter 4

Simulation results and Conclusions

4.1 The pulse collision model validation

The pulse collision model defined in [2],[36] and described in section (2.3.1) provides a possible approach for BER evaluation for an IR-TH-UWB system in the presence of other IR-TH-UWB interfering users. Since the UWB physical layer of our dual physical layer system is a pulse based TH-UWB system, we are particularly interested in adopting the UWB^2 MAC protocol (see section 2.5) that is based on the pulse collision model. As reported in the relative section we are interested in validating simulation results produced by the authors of the model, and more specifically we want to analyze the model behaviour while increasing the number of pulses per bit N_s while maintaining constant the transmitted average power per node P_{TX} and the user data rate R_b, i.e. we vary average pulse repetition period T_s (since $R_b = 1/(N_s \cdot T_s)$). Computer simulations show that increasing N_s provides an higher BER, this is because even if the transmitted average power of different nodes is constant, the useful received energy E_u is reduced due to a shorter average pulse repetition period. In Figure (4.1) three differently populated networks are simulated: as the number of pulses per bit is increased, the system performance in

term of Bit Error Rate slightly worsens.

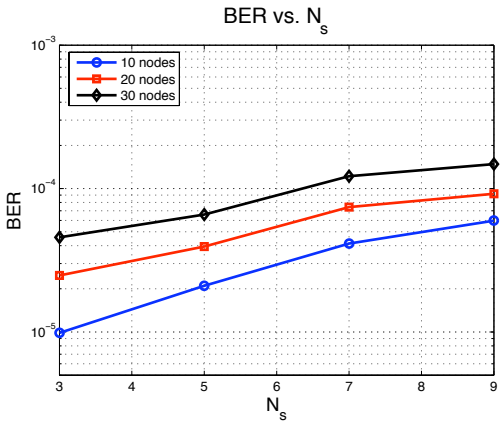

Figure 4.1. BER vs. N_s for different populated networks, according to the pulse collision model increasing N_s does not improve the performance.

With respect to the pulse collision model defined in the literature, we must state that in our simulations we made the hypothesis that even if two packets overlap each other only for an $\epsilon > 0$ amount of time we consider that they collide for the entire packet duration. This is, of course, a worsening hypothesis that was dictated by implementation complexity of the model. The worsening effect of this hypothesis can be highlighted if we simulate an UWB system increasing the number of pulses per bit N_s while maintaining constant the average pulse repetition period T_s. As it is depicted in Figure (4.2), if we increase N_s but fix T_s, we are reducing the bit rate $R_b = 1/(T_s N_s)$, thus a packet with the same length will need more time to be transmitted incrementing the probability of having a packet collision. In the Figure, we show how the number of all interfering packets N_i (sum of the interfering packets perceived by all users) normalized by the number of users in the network and the number of received packets (sum of all packets, desired and interfering, received by all users) increases as N_s increases.

On the other hand if we want the bitrate to remain constant at approximately

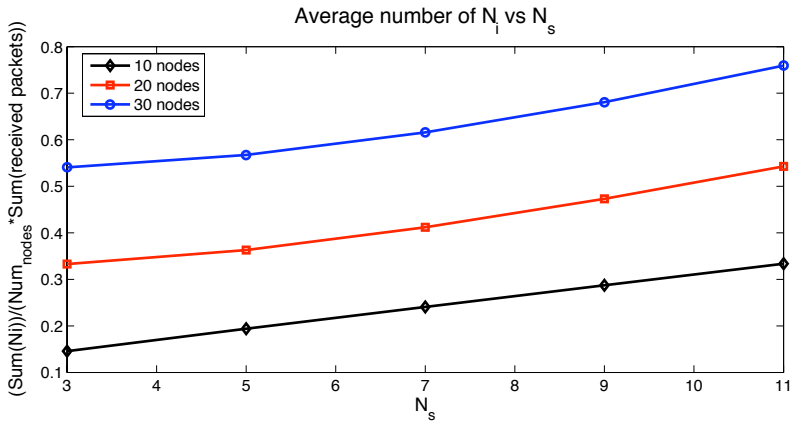

Figure 4.2. Average number of interfering packets N_i as a function of the number of pulses per bit N_s. Maintaining fixed T_s while increasing N_s cause more collisions.

1Mbps, while increasing the number of pulses per bit, the average pulse duration T_s must be reduced accordingly. Figure (4.3) shows how in this case, an higher number of pulses per bit gives the rise to a lower number of interfering packets in the air.

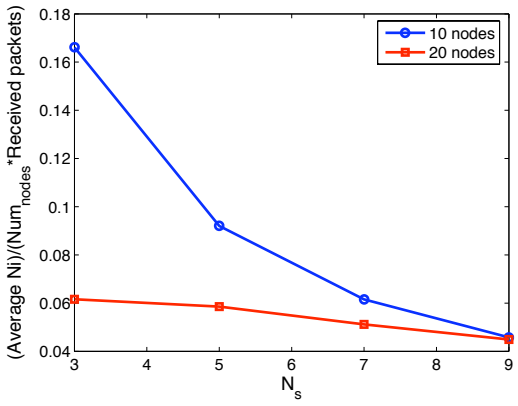

Figure 4.3. Average number of interfering packets N_i as a function of the number of pulses per bit N_s; in this case T_s is reduced with increasing N_s, thus the bitrate R_b remains approximately of 1Mbps.

4.2 Potential Scenarios

The proposed dual physical layer system has several application scenarios that spans from logistics management, industrial control, medical (safety/health) monitoring and others. In general each environment that is characterized by possible high level of interferences or where a degree of confidentiality is needed is a compliant scenario. A particularly interesting use of such a system is for transmissions where Radio Frequencies systems are not welcome, like in hospitals, due to possible interferences with medical equipment. Medical applications are very time-critical and generally involve at least one-way communication of some sort (uplink), however, they may also involve bidirectional communication of data. Even if UWB technology is very robust to narrowband interferers (see section 2.4) and effects of UWB signals onto other systems has very low impacts [37], in some environments RF transmissions are strictly forbidden, moreover the secrecy and safety of critical data like medical reports can be compromised due to possible eavesdroppers. In these cases, a diffuse optical system could be a valid alternative that guarantees absence of interferences with medical equipment and a very high degree of confidentiality. Industrial applications of the proposed model include overall Logistics management Industrial Process Control and Maintenance. Logistics applications generally help improve the efficiency of the operations in which they are used. Finding and tracking are essential elements for these applications, that are less time-critical and generally more tolerant of missed communication (in other words, they can have redundancy built-in with no major impact). Examples include warehouse/supply chain management; package tracking (truck inventory, manifest, proper loading). Industrial Process Control and Maintenance are applications similar to those in industrial inventory control, with the essential difference that at least unidirectional communication (uplink) is a required feature. In these applications, sensors and actuators are generally part of the item being located and the information from the sensors and information to the

actuators needs to be communicated. Examples include wireless sensor networks; large structures monitoring; aircraft/ground vehicle anticollision; and monitoring, sensing and control of industrial and environmental processes.

4.3 Simulated scenario

The simulated environment is an indoor square room of 12mx12m with the ceiling height of 3m. The nodes of the network are always randomly located within the room area and they can be in visibility or not with a certain probability ($NLOS_{probability}$) that is a simulation parameter. The instantaneous transmission rate of each node is supposed to be fixed at $R_b = 966Kbps$, i.e. since $R_b = 1/T_b = 1/(N_s T_s)$, if more than a pulse per bit are transmitted the average pulse repetition time is reduced accordingly. Packets of each node are generated according to a Poisson generation process. The transmitted packet is composed by a payload of 1224 bits and an header of 64 bits that is used by the MAC layer for synchronization issues like described in section (2.5). Since the initial position of the nodes is randomly generated and there is no mobility in the system, all simulations are averaged over 10 runs and each run simulates the network behaviour for 3000 seconds.

The MUI model used in the simulations is the Pulse Collision model (see section 2.3.1) for both UWB and DWO systems. In order to model the impact of channel we adopted the first two channel scenarios defined within the 802.15.4a TG, that is CM1 and CM2, corresponding to indoor Line Of Sight (LOS) and Non-Line Of Sight (NLOS) channel conditions, respectively [44].

The UWB physical layer settings can be summarized as follows:

- IR-UWB with a band of 494 MHz centered at 3952 MHz (corresponding to

Channel 2 of the 802.15.4a channel scheme);

- Average Pulse Repetition Frequency (PRF): 2.895 MHz;
- Pulses Per Symbol (Ns): 3,5 or more;
- Modulation: 2-PPM;
- TX power P_{TX}: fixed to FCC indoor limit [28], leading for the considered bandwidth to $P_{TX} = 36.6\ \mu W$.
- TH-coding with pseudorandom codes.

The presence of narrowband interference (NBI) was also introduced in the UWB physical layer model. The NBI was modeled as an additive white Gaussian noise that sums up with the thermal noise, see section (2.4) for more details. The value of the spectral density of such additional noise depends on the power spectral density and the actual bandwidth of the NBI.

The DWO physical layer settings can be summarized as follows:

- Modulation: OOK;
- Transmitter type: infrared LED $\lambda = 850nm$;
- Pulses Per Symbol (Ns): 1 or more if OOC codes are used;
- TX power P_{TX}: various values from 10^{-4}W to 1W.

4.4 Simulation results

All computer simulations performed in this work were made using the open source discrete event simulation system OMNeT++.

4.4.1 UWB system

Narrow Band Interferences In the presence of narrow band interferers like Fixed Wireless systems, a cellular system or a medical equipment, UWB performance are severely reduced. Even though narrowband signals interfere with only a small fraction of the UWB spectrum, due to their relatively high power with respect to the UWB signal, the performance and capacity of UWB systems can be considerably affected. Figure (4.4) presents the throughput, that is the ratio of the correctly received packets to the total number of received packets, for two different UWB systems one adopting $N_s = 3$ and the other with $N_s = 5$ as a function of the narrow band interferer PSD that is modeled as an additional Gaussian noise.

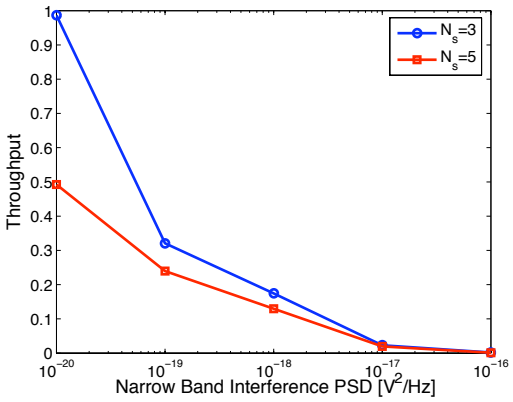

Figure 4.4. Throughput in the case of UWB physical layer with $N_s = 3$ and $N_s = 5$ for a network of 10 nodes with $NLOS_{probability}$=0.3 as a function of the power spectral density of a narrow band interferer N_{NBI}.

For the same scenario of 10 UWB nodes in the presence of narrow band interferers, we can evaluate the energy consumption necessary for the transmission/reception procedures of each node. The function for the evaluation of the energy consumption for a UWB low bitrate system was described in section (3.2.1). As one can reasonably suppose if a narrow band interferer is present each UWB node will be

forced to transmit several times the same packets and consequently perform several times both the transmission and reception procedure. In Figure (4.5) the energy consumption of each node in the presence of narrowband interferers is presented. The average "cost" of transmission is normalized by the number of correctly received packets.

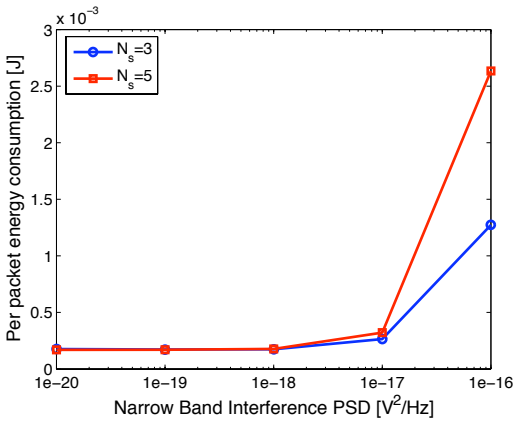

Figure 4.5. Energy consumption for each node of the UWB network as a function of the NBI PSD.

4.4.2 DWO system

According to the modified version of the quantum limit model previously presented, in Figure (4.6) we show the system throughput for two different scenarios, the first with 5 nodes and the second with 10 nodes. In both cases the probability of NLOS links is set to 0.3. Note that with this settings throughput increases when transmitted power increases, however it is clear that if the optical power is higher than 1mW the system saturate in both cases, due to the more and more relevant MUI weight in the error probability formula (3.10).

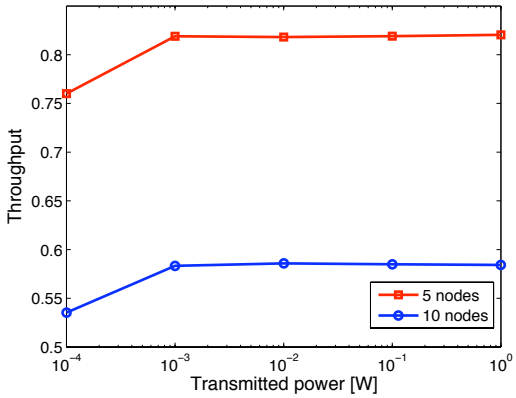

Figure 4.6. Throughput in the case of two differently populated networks with $NLOS_{probability}$ set to 0.3 as a function of the transmitted optical power of the LED.

4.4.3 CIRCUS system

Aimed at defining a system able to switch its physical layer technology from UWB to Optical, we analyzed both systems separately to show how switching from a system to another may conduct to better performance. We exploited previous simulation results and we build up a Figure representing the dual system communicating in an indoor environment. Actually the default technology of current system is the UWB and the transmission is characterized by a TH code and a number of pulses per bit equal to 5. Let this UWB system transmits in the presence of a narrowband interferer with a power spectral density of 10^{-20} $[V^2/Hz]$, current BER value would be approximately $3 \cdot 10^{-5}$. If at the time t_0 another narrowband system characterized by an higher power spectral density of 10^{-6} $[V^2/Hz]$ would enter the same room, performance of the UWB system would instantly worsen. The impact of the ulterior interferer would be the growth of the BER up to a value of about 0.047. In the same scenario an optical diffuse system would not be influenced by RF interferers. Based on the modified quantum limit approach, an optical network with 5 nodes that do

not use any coding, and that transmits with an average power level of 1mW, would obtain a BER of approximately 0.024, that is lower than the UWB BER in the presence of the interferers. In Figure (4.7) we graphically show the behaviour of the dual system in the moment of the technology switching.

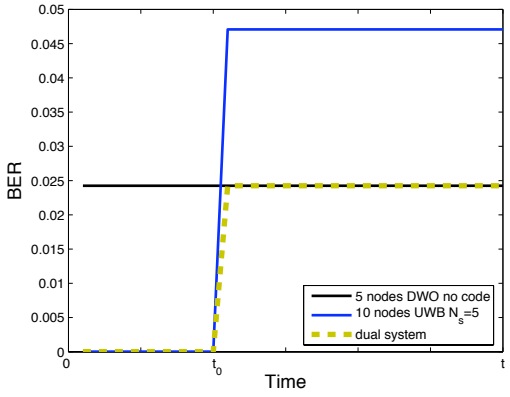

Figure 4.7. An approximation that shows the dual system theoretical behaviour if a narrow band interference would affect the UWB physical part.

4.5 Conclusions

Scope of this thesis work was the investigation of the benefits coming from the convergence of two different impulse-based transmission technologies within a unified system able to switch technology, if necessary. Possible applications of such a system can be low data rate wireless sensor networks that are characterized by the presence of strong radio interference (e.g. industrial settings) and/or severe limitations on the allowed amount of emitted radiations (e.g. medical premises).

We proposed a strategy for selecting the best technology according to the external environment conditions that operates on the basis of BER measurements.

Thanks to the introduction of flexible coefficients in the condition that leads to the selection, different performance goals can be pursued, ranging from simple BER minimization to maximum energy efficiency. Computer simulations analyzed the effectiveness of the combination of the two technologies.

As previously mentioned, accordingly to the defined cost function for the physical layer switching, we investigated a scenario where both the cost coefficients are equal to 1. A deep investigation on the energy consumption evaluation for an optical node, can be a subject of further studies.

Future works can be also oriented on the definition of two "cost" coefficients (one for each physical layer) necessary for the implementation of the second proposed physical layer switching method, the energy optimization. Would be also interesting to study the introduction of Optical Orthogonal Codes and quantify the impact of an increased robustness of the optical part of the system.

Bibliography

[1] J. M. Kahn and J. R. Barry, "Wireless Infrared Communications," *Proceedings of the IEEE*, vol. 85, no. 2, February 1997.

[2] M.-G. DiBenedetto, L. D. Nardis, M. Junk, and G. Giancola, "$(UWB)^2$: Uncoordinated, Wireless, Baseborn, Medium Access Control for UWB communication networks," *Mobile Networks and Applications*, vol. 10, no. 5, pp. 663–674, 2005.

[3] M. D'amico, A. Leva, and B. Micheli, "Free-Space Optics Communication Systems: First Results from a Pilot Field-Trial in the Surrounding Area of Milan, Italy," *IEEE Microwave and Wireless Components Letters*, vol. 13, no. 8, pp. 305–307, August 2003.

[4] H. A. Willebrand and B. S. Ghuman, "Fiber optics without fiber," *Spectrum, IEEE*, vol. 38, no. 8, pp. 40–45, August 2001.

[5] Communication by Light CBL. [Online]. Available: http://www.cbl.de/englisch/

[6] F. Gfeller and U. Bapst, "Wireless in-house data communication via diffuse infrared radiation," *Proceedings of the IEEE*, vol. 67, no. 11, pp. 1474–1486, november 1979.

[7] J. Carruthers, "Wireless infrared communications," Wiley Encyclopedia of Telecommunications, 2002.

[8] K. Langer and J. Grubor, "Recent developments in optical wireless communications using infrared and visible light," ICTON, 2007.

[9] R. Matsuo, M. Matsuo, T. Ohtsuki, T. Udagawa, and I. Sasase, "Performance analysis of indoor infrared wireless systems using ook cdma on diffuse channels," 1999.

[10] J. R. Barry, J. M. Kahn, W. J. Krause, E. A. Lee, and D. G. Messerschmitt, "Simulation of multipath impulse response for indoor wireless optical channels," *IEEE Journal on Selected Areas in Communications*, vol. 11, no. 3, pp. 367–379, April 1993.

[11] F. J. Lopez-Hernandez, E. Poves, R. Perez-Jimenez, and J. Rabadan, "Low-Cost Diffuse Wireless Optical Communication System based on White LED," *ISCE '06. 2006 IEEE Tenth International Symposium on Consumer Electronics*, no. 1-4, 2006.

[12] M. Audeh and J. Kahn, "Performance Evaluation of Baseband OOK for Wireless Indoor Infrared LANs Operating at 100 Mb/s," *IEEE Transactions on Communications*, vol. 43, no. 6, pp. 2085–2094, June 1995.

[13] U. N. Griner and S. Arnon, "Multiuser Diffuse Indoor Wireless Infrared Communication Using Equalized Synchronous CDMA," *IEEE Transactions on Communications*, vol. 54, no. 9, pp. 1654–1662, September 2006.

[14] S. Han, "Optical CDMA with Optical Orthogonal Code," Multiuser Wireless Communication, 2002.

[15] F. R. K. Chung, J. A. Salehi, and V. K. Wei, "Optical Orthogonal Codes: Design, Analysis, ans Applications," *IEEE Transactions on Information Theory*, vol. 35, no. 3, p. 595604, May 1989.

[16] M. Choudhary, P. K. Chatterjee, and J. John, "Optical Orthogonal Codes Using Error Correcting Codes," 2002.

[17] The LEOT curriculum by the Center for Occupational Research and

Development (CORD). [Online]. Available: http://cord.org/cm/content1.htm

[18] J. MacChesney, "Fiber optics tutorial, Bell Labs, Lucent Technologies." [Online]. Available: http://www.arcelect.com/fibercable.htm

[19] B. E. A. Saleh and M. C. Teich, F*undamentals of* P*hotonics*. Wiley-Interscience, 1991.

[20] D. Kedar and S. Arnon, "Urban optical wireless communication networks: the main challenges and possible solutions," *IEEE Communications Magazine*, vol. 42, no. 5, pp. S2–S7, May 2004.

[21] X. Zhu and J. M. Kahn, "Free-Space Optical Communication through Atmospheric Turbolence Channels," *IEEE Transactions on Communications*, vol. 50, no. 8, pp. 1293–1300, August 2002.

[22] S. Hranilovic, W*ireless* O*ptical* C*ommunication* S*ystems*, 1st ed. Springer, September 2004.

[23] J. Carruthers, S. Carroll, and P. Kannan, "Propagation modelling for indoor optical wireless communications using fast multi-receiver channel estimation," *Optoelectronics, IEEE Proceedings*, vol. 150, no. 5, pp. 473–481, October 2003.

[24] J. B. Carruthers and J. M. Kahn, "Modeling of Nondirected Wireless Infrared Channels," *IEEE Transactions on Communications*, vol. 45, no. 10, pp. 1260–1268, October 1997.

[25] A. Sato, M. Asano, H. Uehara, and I. Sasase, "The Iinfluence of Multipath Distortion on the Transmitted Pulse in Diffuse Indoor Infrared Channels," C*omputer and* S*ignal* P*rocessing* C*ommunications*, vol. 2, no. 636-639, August 1997.

[26] A. J. C. Moreira, R. T. Valadas, and A. M. de Oliveira-Duarte, "Optical interference produced by artificial light," *Wirel. Netw.*, vol. 3, no. de Oliveira Duarte A.M., pp. 131–140, 1997.

[27] V. Vitsas and A. C. Boucouvalas, "Performance analysis of the advanced infrared (Air) CSMA/CA MAC protocol for wireless LANs," *Wirel. Netw.*, vol. 9, no. 5, pp. 495–507, 2003.

[28] FCC, "Revision of part 15 of the commission's rules regarding ultra-wideband transmission systems," First Report and Order, ET Docket 98-153, FCC 02-8, adopted/ released, February 2002.

[29] H. F. Harmuth, *Transmission of Information by Orthogonal Functions*, 1st ed. Springer, 1969.

[30] G. F. Ross, "A time domain criterion for the design of wideband radiating elements," *IEEE Trans. on Antennas and Propagation*, vol. 16, no. 335, 1968.

[31] T. W. Barrett, "Hystory of ultra wide band (UWB) radar & communications: Pioneers and Innovators," Pogress In Electromagnetics Symposium, July 2000.

[32] "Assessment of Ultra-Wideband (UWB) technology," OSD/DARPA, Ultra-Wideband Uadar Review Panel, R-6280, July 1990.

[33] L. Yang and G. B. Giannakis, "Ultra-Wideband Communications an Idea Whose Time Has Come," IEEE Signal Processing Magazine, November 2004.

[34] M.-G. DiBenedetto and G. Giancola, U*nderstanding* U*ltra* W*ide* B*and* R*adio* F*undamentals*. Prentice Hall, 2004.

[35] M.-G. DiBenedetto and B. R. Vojcic, "Ultra Wide Band UWB Wireless Communications: A Tutorial," *Journal of Communication and Networks, Special Issue on Ultra-Wideband Communications*, vol. 5, no. 4, pp. 290–302, December 2003.

[36] G. Giancola and M.-G. DiBenedetto, "A novel approach for estimating multi-user interference in impulse radio UWB networks: The pulse collision model," Signal Processing, Special Issue on Signal Processing in UWB Communications. Invited paper, pp. 2185–2197, 2006.

[37] R. Giuliano and F. Mazzenga, "On the Coexistence of Power-Controlled

Ultrawide-Band Systems With UMTS, GPS, DCS1800, and Fixed Wireless Systems," *IEEE Transactions on Vehicular Technology*, vol. 54, no. 1, pp. 62–81, January 2005.

[38] H. Arslan, Z. N. Chen, and M.-G. DiBenedetto, Eds., *Ultra Wideband Wireless Communication*. Wiley-Interscience, 2006.

[39] M. E. Sahin and H. Arslan, "A narrowband interference identification approach for UWB systems," *Military Communications Conference, MILCOM*, vol. 3, pp. 1404–1408, October 2005.

[40] "Ieee 802.15.4 MAC standard." [Online]. Available: http://www.ieee802.org/15/pub/TG4.html

[41] R. Min and Chandrakasan, "A Framework for Energy-Scalable Communication in High-Density Wireless Networks," *International Symposium on Low Power Electronics and Design (ISLPED)*, no. 36-41, 2002.

[42] E. A. Lee and D. G. Messerschmitt, *Digital Communication*. Norwell, MA 02061, USA: Kluwer Academix Publishers, 1988.

[43] Y. Alqudah, M. Kavehrad, and S. Jivkova, "Optical wireless multispot diffusing: a MIMO configuration," *Communications, 2004 IEEE International Conference on*, vol. 6, pp. 3348–3352, June 2004.

[44] "Ieee 802.15.4a channel model final report, rev.1 (november 2004)." [Online]. Available: ftp://ieee:wireless@ftp.802wirelessworld.com/15/04/15-04-0662-00-004a-channel-model-final-report-r1.pdf